Time scales, persistence, and dynamic multiscaling in homogeneous, isotropic fluid turbulence

Rahul Pandit

Centre for Condensed Matter Theory
Department of Physics
Indian Institute of Science
Bangalore, India.

19 October 2011
NORDITA, Stockholm.

Many happy returns of the day!

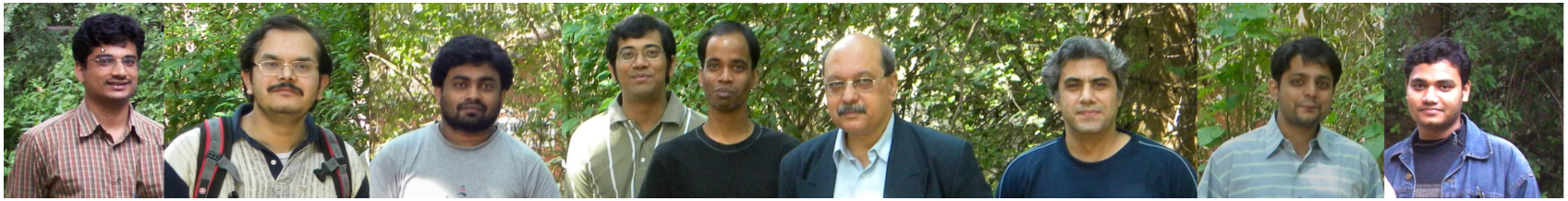

- This work has been done with
  - Dhrubaditya Mitra
  - Prasad Perlekar
  - Samriddhi Sankar Ray
- Support: CSIR, DST, UGC (India) and SERC (IISc)

References

- *Dynamic Multiscaling in Fluid Turbulence : An Overview,* D. Mitra and R. Pandit, *Physica A* **318**, 179 (2003).
- *Varieties of Dynamic Multiscaling in Fluid Turbulence,* D. Mitra and R. Pandit. *Phys. Rev. Lett.* **93**, 024501 (2004).
- *Dynamics of Passive-Scalar Turbulence,* D. Mitra, R. Pandit, *Phys. Rev. Lett.* **95**, 144501 (2005).
- *Dynamic Multiscaling in Turbulence*, R. Pandit, S. S. Ray, and D. Mitra, *Eur. Phys. J. B* **64**, 463 (2008).
- *The Universality of Dynamic Multiscaling in Homogeneous, Isotropic Navier-Stokes and Passive-Scalar Turbulence*, S. S. Ray, D. Mitra, and R. Pandit, *New J. of Phys.* **10**, 033003 (2008).
- *The Persistence Problem in Two-Dimensional Fluid Turbulence*, P. Perlekar, S. S. Ray, D. Mitra, and R. Pandit, *Phys. Rev. Lett.* **106**, 054501 (2011).
- *Dynamic Multiscaling in Two-dimensional Turbulence*, S. S. Ray, D. Mitra, P. Perlekar, and R. Pandit, *Phys. Rev. Lett.*, in press.

Preview

- Long residence time of tracers in vortical regions.
- $\tau_\ell \sim \ell^z$
  - K41: $\tau_\ell \sim \ell / v_\ell \sim \ell^{2/3} \Rightarrow z^{K41} = 2/3$.
  - Mean flow: $\ell = U\tau_\ell \Rightarrow z = 1$ (Heisenberg and Onsager).

Outline

- Two-dimensional turbulence in soap films :
  - Persistence
- Multiscaling in homogeneous, isotropic, turbulence:
  - Structure functions;
  - Kolmogorov 1941 - simple scaling;
  - Multiscaling and dynamic multiscaling.
- Conclusions.

Two-dimensional turbulence in soap films.

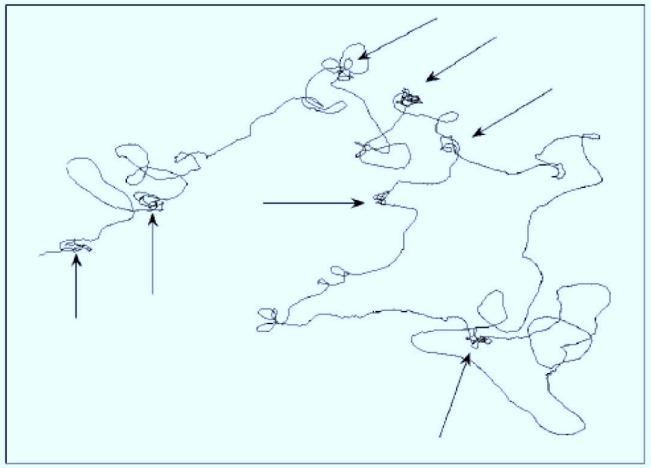

FIG. 5. Typical trajectory of a single particle. The solid line represents the part of the trajectory that corresponds to a trap while a dashed line corresponds to a flight between traps.

O. Cardoso, B. Gluckmann, O. Parcollet, and P. Tabeling, Phys. Fluids **8** (1), 1996.

Two-dimensional turbulence:

- Study of high-Reynolds-number solution of the incompressible Navier-Stokes equations:

$$D_t \mathbf{u} = -\nabla p + \nu \nabla^2 \mathbf{u}, \qquad (1)$$
$$\nabla . \mathbf{u} \equiv 0$$

or

$$\begin{aligned} D_t \omega &= \nu \nabla^2 \omega, \qquad (2) \\ \nabla^2 \psi &= \omega, \\ \omega &\equiv \nabla \times \mathbf{u}, \\ u_x &= -\partial_y \psi, \\ u_y &= \partial_x \psi. \end{aligned}$$

- No vortex stretching, $\omega . \nabla \mathbf{u}$ is absent.

Conservation laws:

- Energy conservation in the inviscid, unforced limit.

$$\partial_t E = -2\nu\Omega, \tag{3}$$

$$E = 1/2 \int_{\mathbf{x}\in R^3} |\mathbf{u}|^2,$$

$$\Omega = 1/2 \int_{\mathbf{x}\in R^3} |\omega|^2, \tag{4}$$

- Enstrophy conservation in the inviscid, unforced limit.

$$\partial_t \Omega = -2\nu P, \tag{5}$$

$$P = 1/2 \int_{\mathbf{x}\in R^3} |\nabla \times \omega|^2. \tag{6}$$

Cascades

[Kraichnan, Phys. Fluids, **10**, (1967*a*), Batchelor, Phys. Fluids Suppl. *II*, **12**, (1969)]

- Energy injected at a length scale l_{inj} will inverse-cascade to large length scales with $E(k) \sim k^{-5/3}$.
- Energy injected at a length scale l_{inj} will forward-cascade to small length scales with $E(k) \sim k^{-3}$.

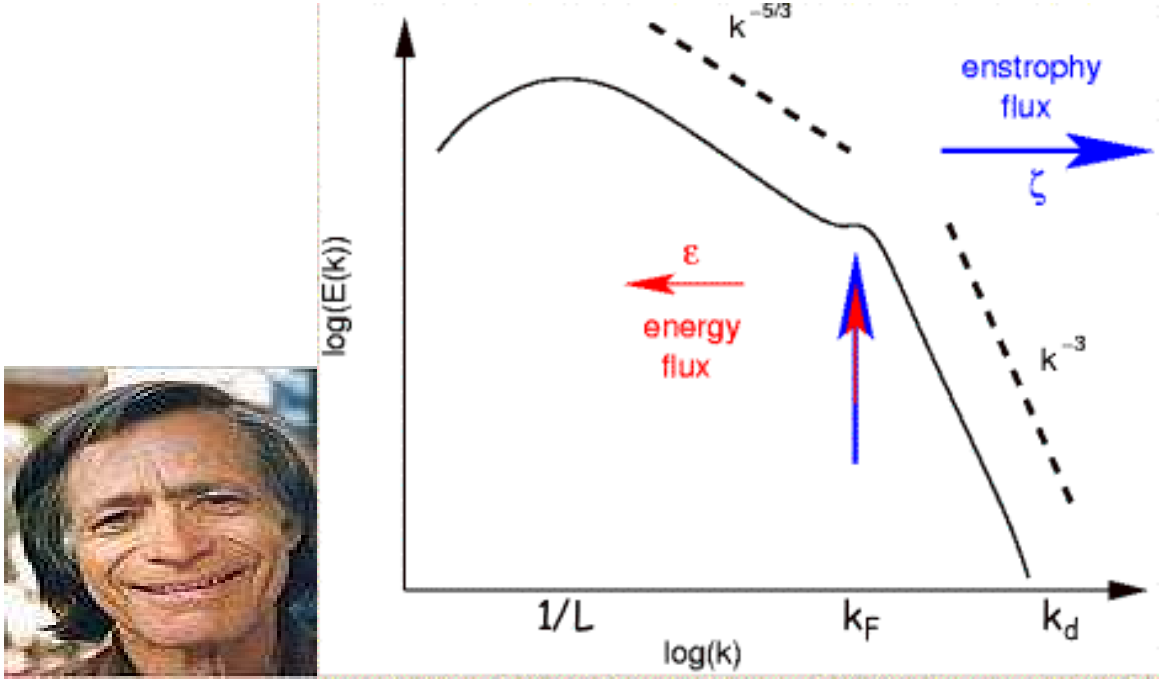

Electromagnetically forced soap films

[M. Rivera, Ph.D. Thesis, arXiv:physics/010305v1]

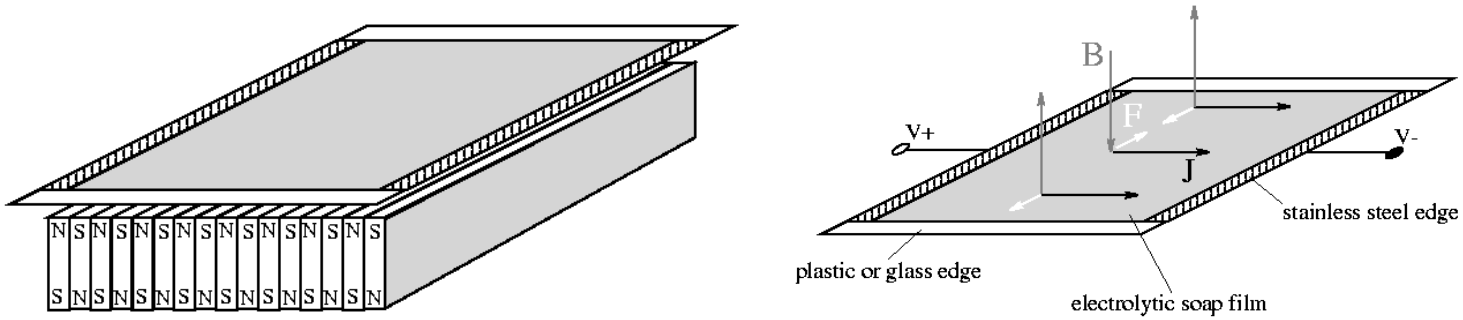

- Soap film: $400ml$ distilled water $+$ $40ml$ glycerol $+$ $5ml$ commercial liquid detergent,
- The soap film is suspended on a rectangular frame,
- The magnetic array produces a Kolmogorov forcing $F_x = F_0 sin(k_y y)$.

Modelling soap films: Incompressible limit

[Chomaz et al., PRA, **41**, (1990), Chomaz, JFM, (2001), P. Fast, arXiv:physics/0511175v1, (2005).]

- Mach Number $M_e \equiv u_{rms}/c$, where c is the speed of the sound in the soap films. For the experiments with electromagnetically forced soap films $M_e \sim 0.06$.
- To leading order soap-film behaviour is governed by the Navier-Stokes (NS) equations in two dimensions + an air drag

$$\begin{aligned} D_t \mathbf{u} &= \nu \nabla^2 \mathbf{u} - \nabla p - \alpha \mathbf{u}, \\ \nabla \cdot \mathbf{u} &= 0. \end{aligned}$$

- $D_t \equiv \partial_t + \mathbf{u} \cdot \nabla$, $p \equiv$ pressure, and $\mathbf{u} \equiv$ the velocity

Direct Numerical Simulation(DNS)

- Vorticity-streamfunction formulation:

$$
\begin{aligned}
D_t\omega &= \nu\nabla^2\omega - \alpha\omega, \\
\nabla^2\psi &= \omega, \\
u_x &= -\partial_y\psi, u_y = \partial_x\psi.
\end{aligned}
$$

- Incompressibility satisfied by construction.
- No-slip boundary condition on the walls.

DNS for forced soap films:

- Impose the Kolmogorov forcing $F_y = F_0 \sin(k_x x)$ at all times.
- Study the evolution of the energy E and the dissipation rate ϵ with α and ν.
- Study velocity and vorticity structure functions.
- Study the topological properties via PDFs of the Weiss parameter Λ.

Evolution of energy and dissipation

Time evolution of $E(t)/E'$ [(a) and (b)], $\epsilon(t)/\epsilon'$ [(c) and (d)] , and $\epsilon_e(t)/\epsilon'$ [(e) and (f)].

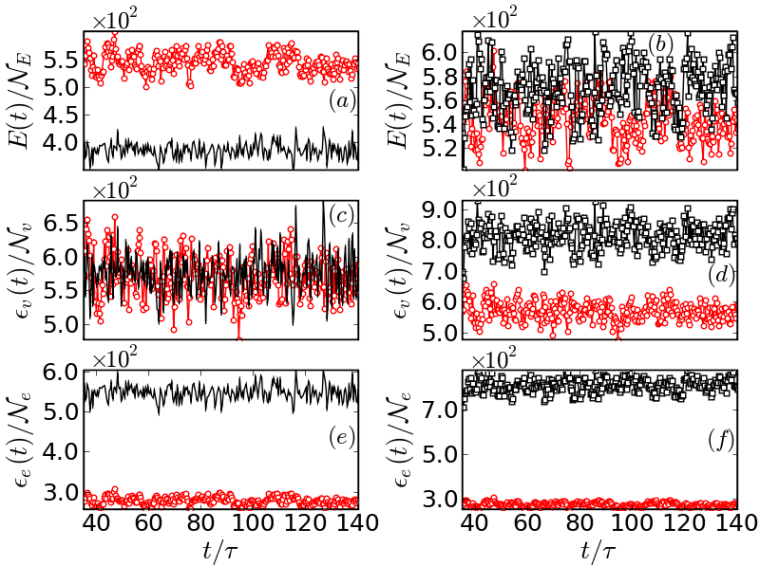

In (a), (c), and (d) we keep $\mathcal{G}$ fixed and vary γ ($\gamma = 0.25$(red lines with circles) and $\gamma = 0.71$(black line)). In (b), (d), and (f) we maintain $Re \simeq 21.2$ and vary γ ($\gamma = 0.25$(red lines with circles) and $\gamma = 0.71$(black line with squares)).

Pseudocolor plots

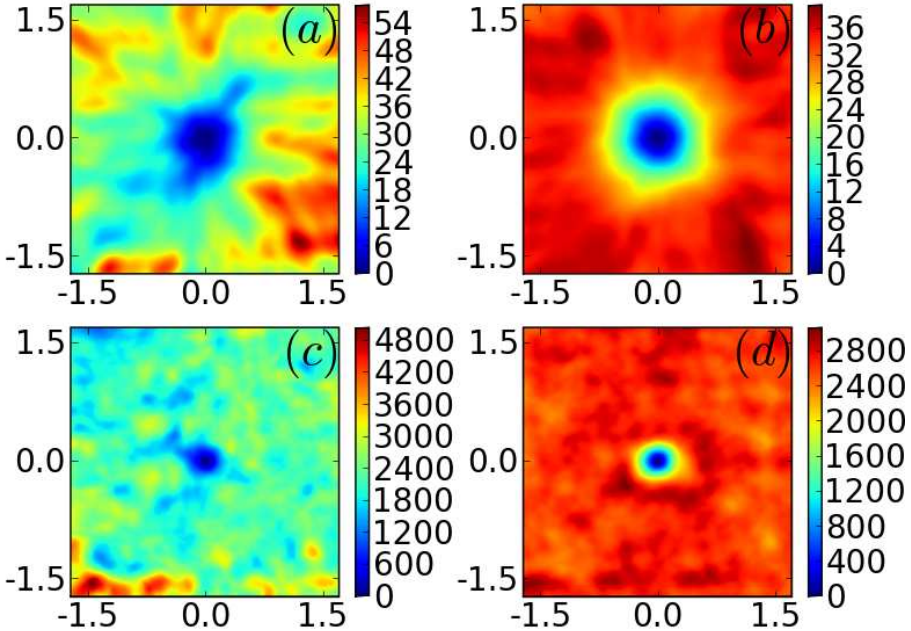

Pseudocolor plots of (a) $S_2(\mathbf{r_c}, \mathbf{R})$, for $\mathbf{r_c} = (2, 2)$, (b) $S_2(R)$ (average of $S_2(\mathbf{r_c}, \mathbf{R})$ over $\mathbf{r_c}$), (c) $S_2^{\omega}(\mathbf{r_c}, \mathbf{R})$, for $\mathbf{r_c} = (2, 2)$, and (d) $S_2^{\omega}(R)$ (average of $S_2^{\omega}(\mathbf{r_c}, \mathbf{R})$ over $\mathbf{r_c}$).

Velocity Structure Functions

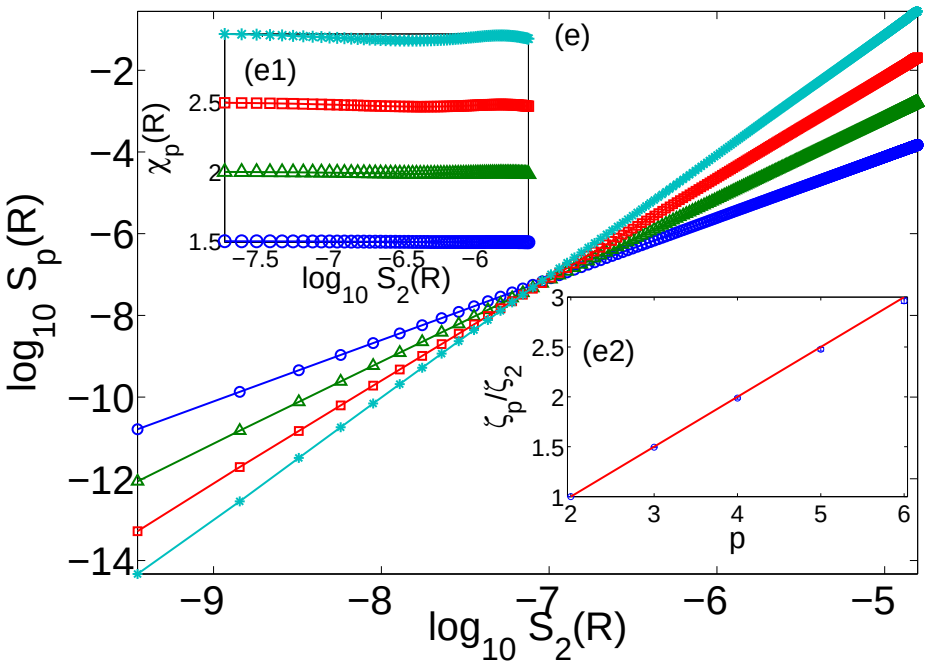

Vorticity Structure Functions

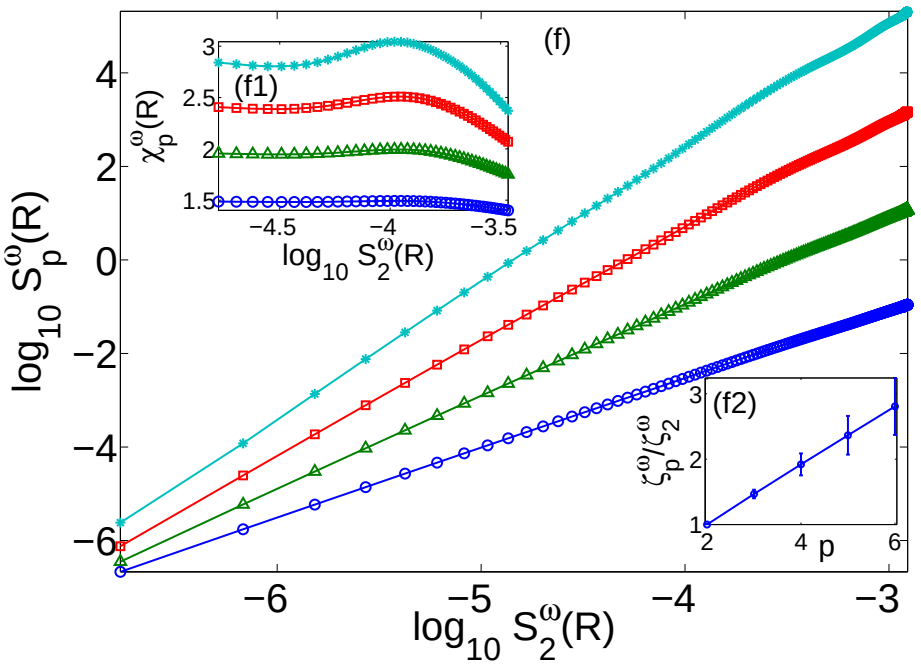

Distribution of centers and saddles

A. Okubo, Deep-Sea Res. **17**, 17 (1970),
J. Weiss, Physica, **48D**, 273 (1991).

- Local flow topology determined by

$$\Lambda \equiv \begin{vmatrix} \partial_x u_x & \partial_x u_y \\ \partial_y u_x & \partial_y u_y \end{vmatrix} \textit{and}$$

  $D \equiv \nabla \cdot \mathbf{u}$

- For incompressible flows, $D = 0$
- $\Lambda = (\omega^2 - \sigma^2)/4$, $\omega^2 \equiv \sum_{i,j} (\partial_i u_j - \partial_j u_i)^2/2$, $\sigma^2 \equiv \sum_{i,j} (\partial_i u_j + \partial_j u_i)^2/2$.
- At a point (x, y), $\Lambda(x, y) > 0 \implies$ centers, and $\Lambda(x, y) < 0 \implies$ saddles.

ψ and Λ

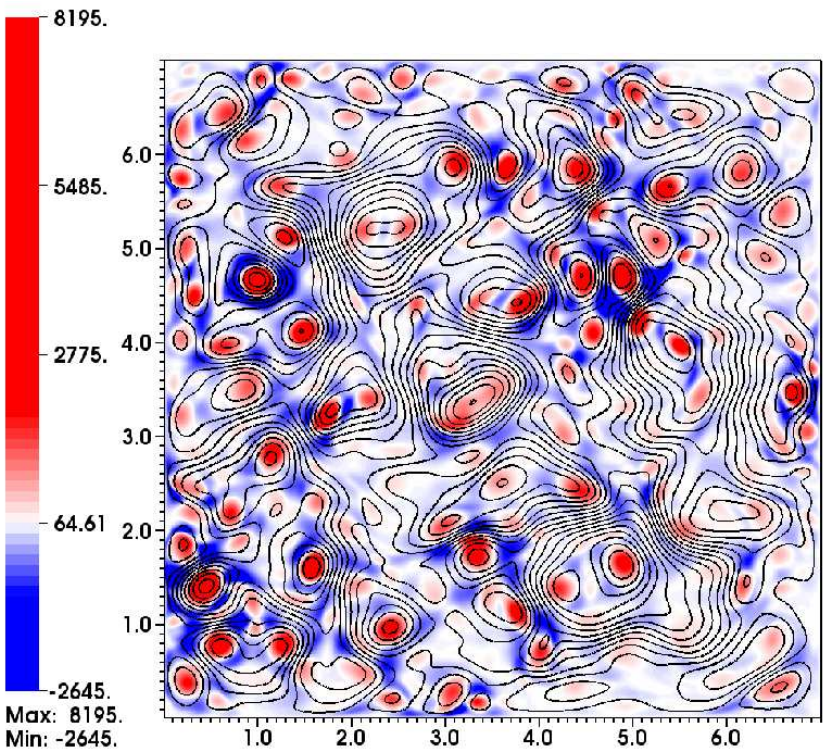

- Contours of ψ overlayed on the pseudocolor plot of Λ.
- $\Lambda > 0$(centers)
- $\Lambda < 0$(saddles)

PDF of Λ: fixed Re

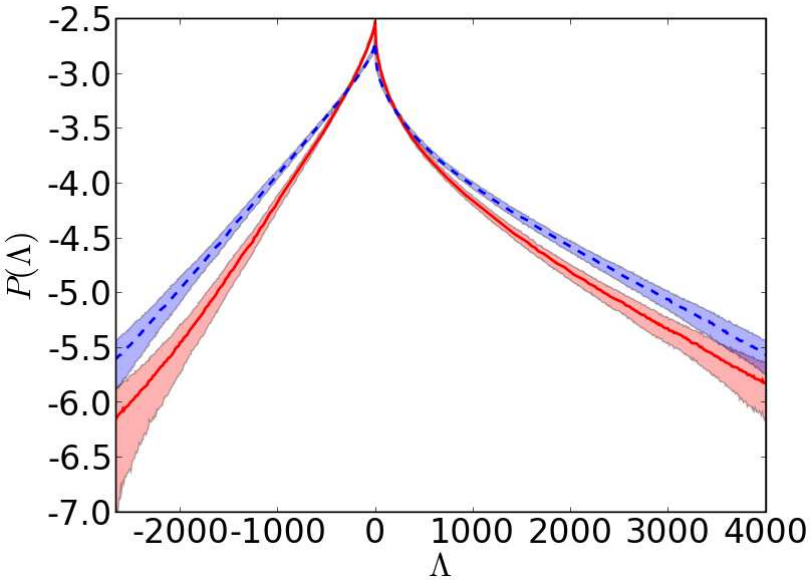

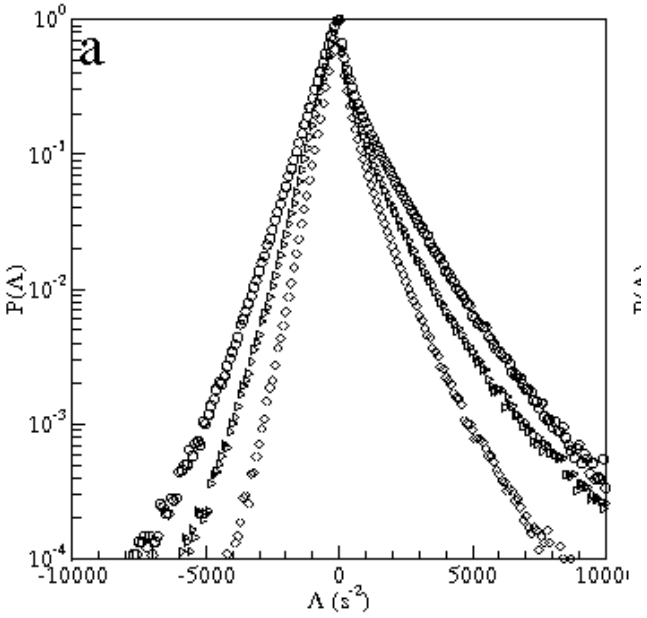

- runs R4 and R6
- Left: Our DNS. $\gamma = 0.25(red)$, $\gamma = 0.71(blue)$.
- Right: Experiments. $\gamma = 0.28$(diamond), $\gamma = 0.56$(triangle), $\gamma = 0.97$(circle).

PDF of Λ: fixed Re

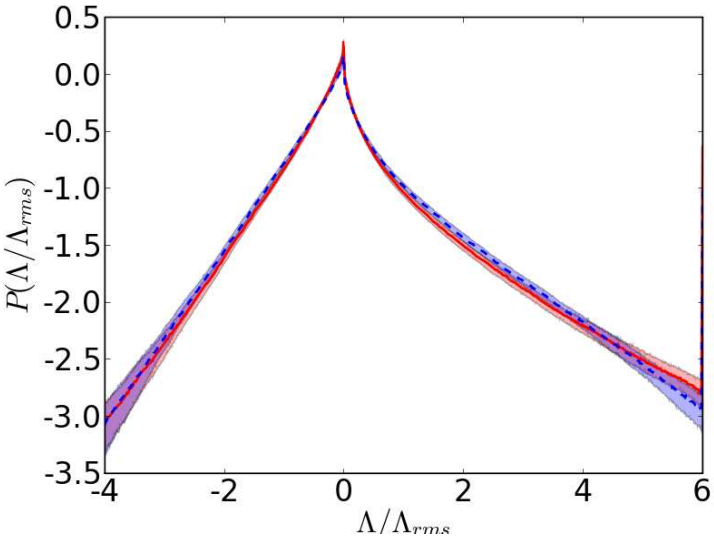

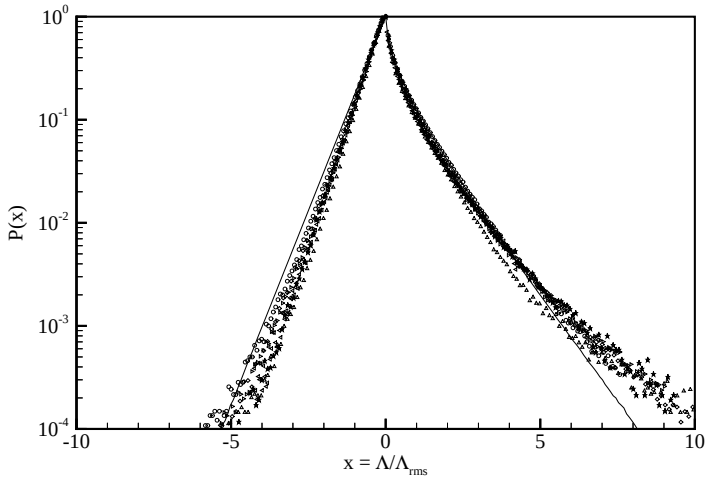

- runs R4 and R6
- PDF normalized by Λ_{rms}.
- Left: Our DNS. $\gamma = 0.25(red)$, $\gamma = 0.71(blue)$.
- Right: Experiments. $\gamma = 0.28$(diamond), $\gamma = 0.56$(triangle), $\gamma = 0.97$(circle).

Persistence problem

- Satya N. Majumdar, Persistence in Nonequilibrium Systems, Curent Science, **77**, 370 (1999); cond-mat/9907407v1
  Let $\phi(x,t)$ be a nonequilibrium field fluctuating in space and time according to some dynamics. Persistence is simply the probability $P_0(t)$ that, at a fixed point in space, the quantity $sgn[\phi(x,t) - \langle\phi(x,t)\rangle]$ does not change upto time t.
- $P^{\phi}(\tau) \sim \tau^{-\beta}$ as $\tau \to \infty$, where β is the *persistence exponent*.

The Okubo-Weiss parameter

- From the velocity-gradient tensor $\mathcal{A}$, with components $A_{ij} \equiv \partial_i u_j$, we obtain the Okubo-Weiss parameter Λ, the discriminant of the characteristic equation for $\mathcal{A}$.
- If Λ is positive (negative) then the flow is vortical (extensional).
- In an incompressible flow in two dimensions $\Lambda = \det\mathcal{A}$; and the PDF of Λ has been shown to be asymmetrical about $\Lambda = 0$ (vortical regions are more likely to occur than strain-dominated ones).

Motivation

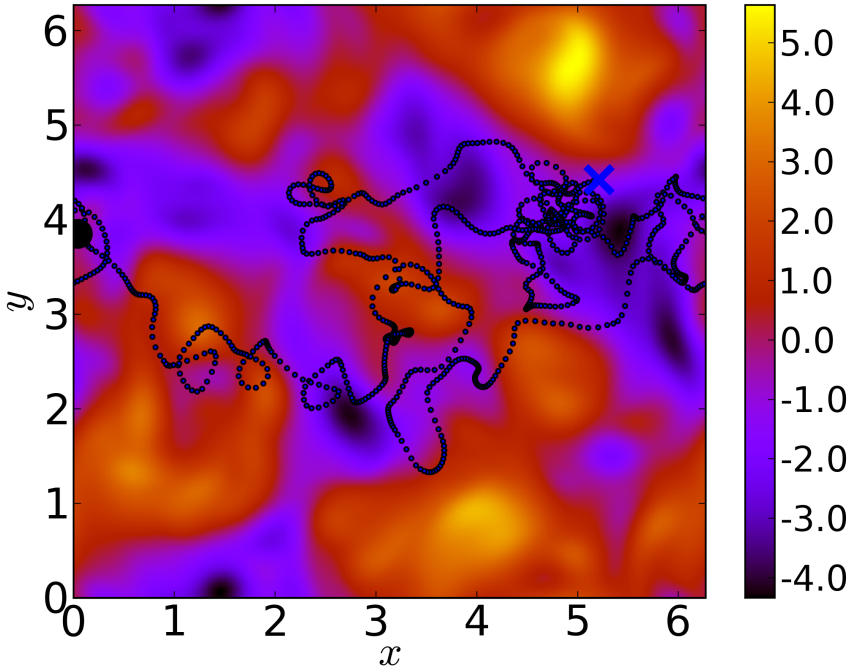

- Note $\langle \Lambda \rangle = 0$.
- How long does a Lagrangian particle stay in region where $\Lambda > 0$ (center) or where $\Lambda < 0$ (saddle).
- How long does the Λ field not change sign at a position (x, y) i.e., persistence time of a center or a saddle.

Persistence in two-dimensional turbulence

- Lagrangian persistence: We follow N_p particles and evaluate Λ along their trajectories.
- Eulerian persistence: We monitor the time evolution of Λ at N positions in the simulation domain.
- For both the cases we find the time-intervals τ over which $\Lambda > 0$ or $\Lambda < 0$. The PDF of these intervals characterizes the analog of persistence in two dimensional turbulence.

Persistence-time PDF

- We denote the persistence-time PDFs by P; the subscripts E and L on these PDFs signify Eulerian and Lagrangian frames, respectively; and the superscripts $+$ or $-$ distinguish PDFs from vortical points from those from extensional ones.
- To find out the persistence-time PDF $P_E^+(\tau)$ [resp., $P_E^-(\tau)$] we analyse the time-series of Λ obtained from each of the N_p Eulerian points and construct the PDF of the time-intervals τ over which Λ remains positive (resp., negative).
- The same method applied to the time series of Λ, obtained from each of the N_p Lagrangian particles, yields $P_L^+(\tau)$ [resp., $P_L^-(\tau)$].

Simulation details

N	ν	μ	F_0	k_{inj}	l_d	λ	Re_λ	T_{E}^{-}	T_{L}^{-}	T_{E}^{+}
512	0.016	0.1	45	10	0.023	0.17	59.2	0.6	0.12	0.34
512	0.016	0.45	45	10	0.021	0.11	26.8	0.4	0.15	0.28
1024	10^{-5}	0.01	0.005	10	0.0043	0.125	827.3	20.0	9.9	14.28
1024	10^{-5}	0.01	0.005	4	0.0054	0.198	1318.8	33.3	12.5	25.0

Time series of Λ

Lagrangian versus Eulerian frame

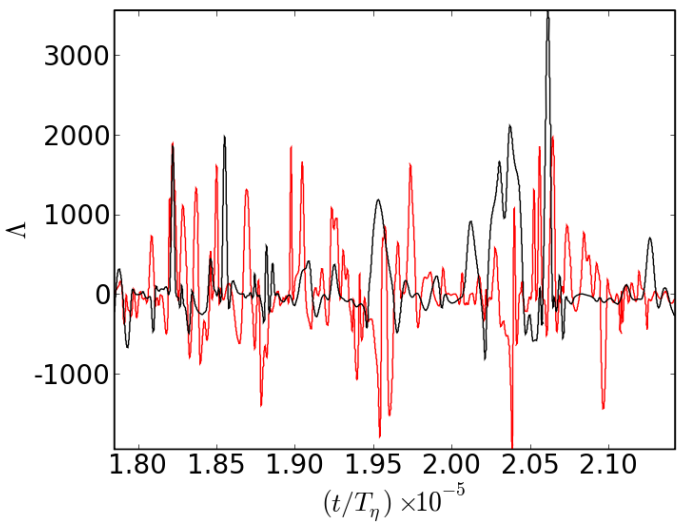

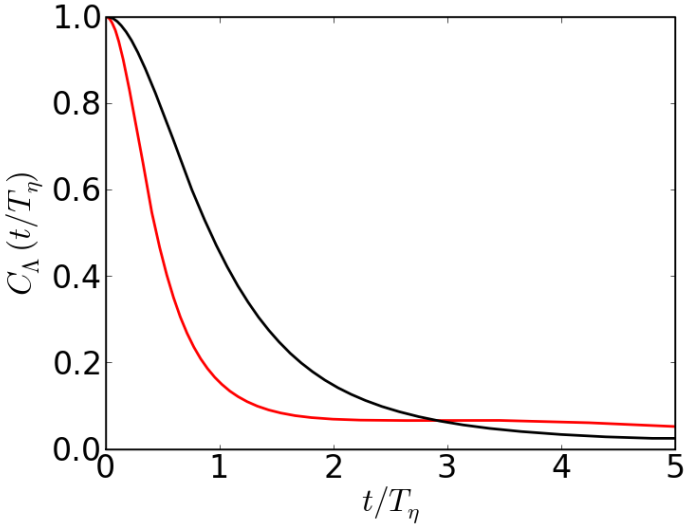

- Lagrangian Λ tracks (red) show rapid fluctuations in comparison to the corresponding Eulerian tracks (black).
- Autocorrelation $C_\Lambda = \langle \Lambda(t_0)\Lambda(t_0+t)\rangle$ decays faster for the Lagrangian case.

Persistence: particle in a vortex

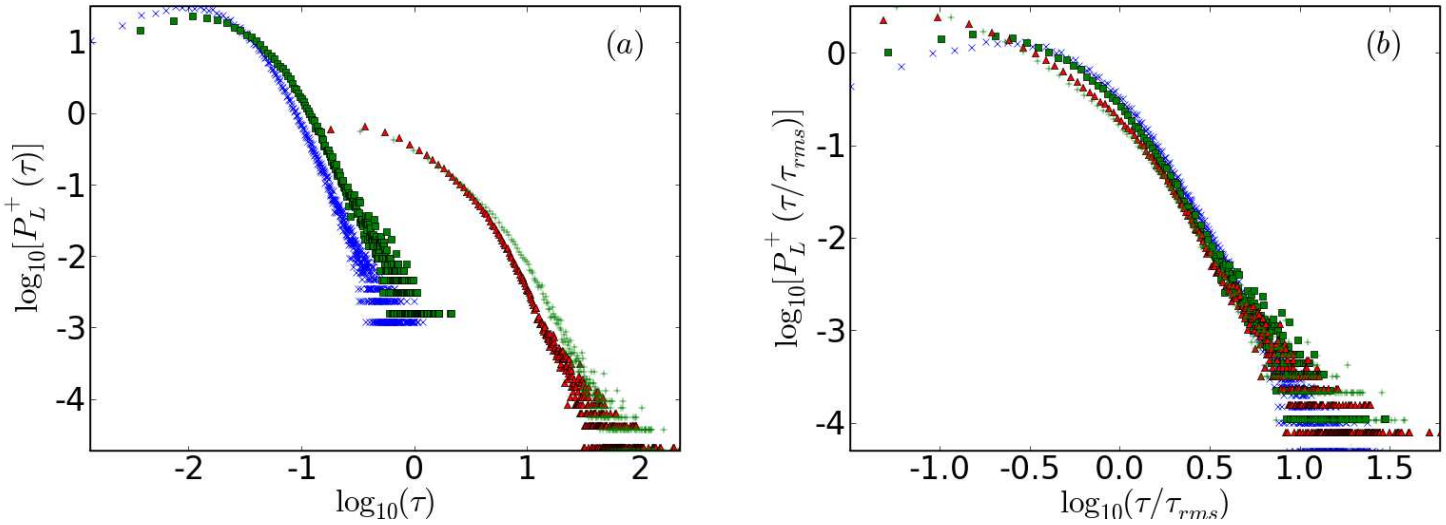

- $Re = 59.2,\ k_{inj} = 10,\ \alpha = 0.1$ ($\times$),
- $Re = 26.8,\ k_{inj} = 10,\ \alpha = 0.45$ ($\square$),
- $Re = 827.3,\ k_{inj} = 4,\ \alpha = 0.01$ ($\triangle$),
- $Re = 1318.8,\ k_{inj} = 10,\ \alpha = 0.01$ ($+$).

Persistence: particle in a vortex

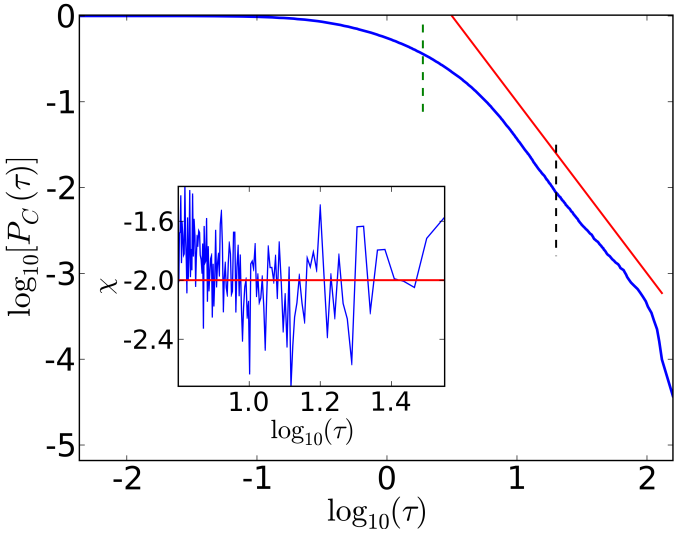

- $P^C(\tau) = \tau^{-(\beta-1)}$, $\beta = 2.9 \pm 0.2$.
- Independent of Re, k_{inj}, and α

Persistence: particle in a region of strain

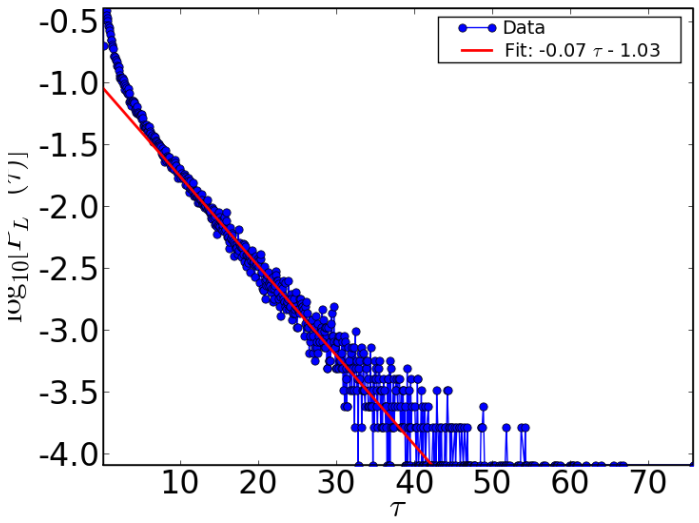

- Lin-log plot of the persistence time of the particle in a region of strain.

Persistence: Region of vorticity at (x, y)

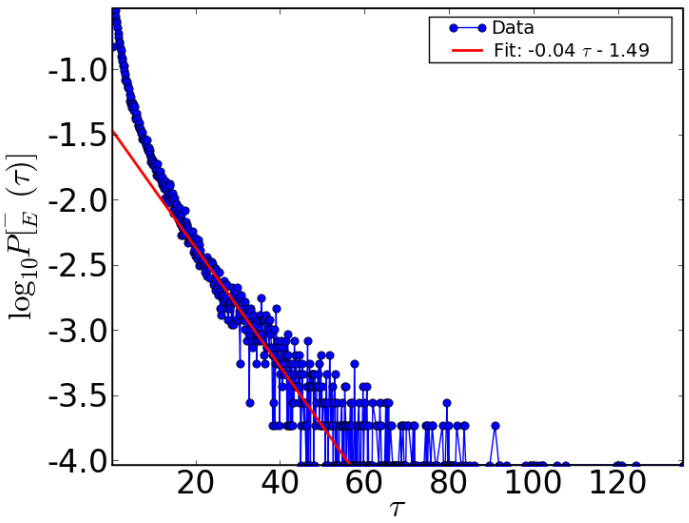

- Lin-log plot of the persistence time of the region of vorticity at position (x, y).

Persistence: Region of strain at (x, y)

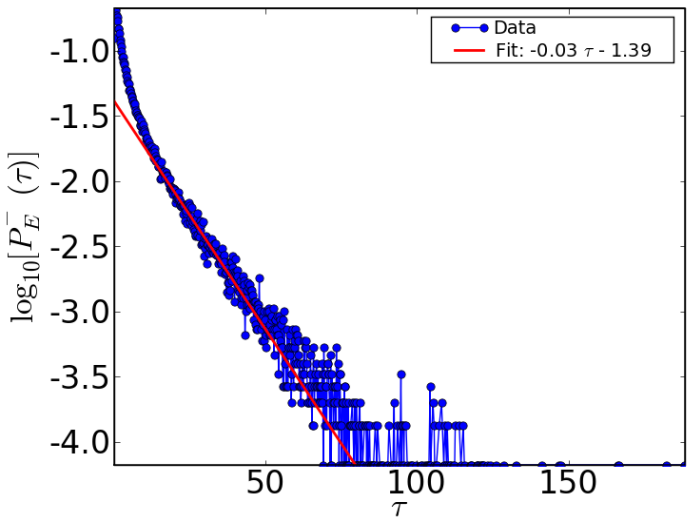

- Lin-log plot of the persistence time of the region of strain at position (x, y).

Conclusion

- The Okubo-Weiss parameter provides us with a natural way of formulating and studying the persistence problem in two-dimensional fluid turbulence.
- The persistence-time PDF of Lagrangian particles in vortical and strain-dominated regions are different.
- The persistence-time PDF of Lagrangian particles in vortical regions show a power-law tail with an exponent $\beta = 2.9$.
- The persistence-time PDF of Lagrangian particles in strain-dominated regions shows an exponential tail.

Multiscaling in Fluid and Passive-Scalar Turbulence

Multiscaling in homogeneous, isotropic, turbulence:

- Structure functions;
- Kolmogorov 1941 - simple scaling;
- multiscaling and dynamic multiscaling;
- passive-scalar turbulence.

Critical Phenomena

$\Gamma(r,t,h) \approx \frac{1}{r^{d-2+\eta}}\mathcal{F}(t^{\nu}\xi, h/t^{\Delta})$

- r: separation between the spins in d dimensions
- $t \equiv (T - T_c)/T_c$
- $h \equiv H/k_B T_c$
- k_B: Boltzmann constant
- T: temperature
- T_c: critical temperature
- H: magnetic field
- ξ: correlation length (diverges at criticality)
- η, ν and Δ: static critical exponents
- $\mathcal{F}$: universal scaling function

Critical Phenomena

In Fourier space
$\tilde{\Gamma}(q,t,h) \approx \frac{1}{q^{2-\eta}}\mathcal{F}(t^{\nu}\xi, h/t^{\Delta})$;
$\vec{q}$: wave vector with magnitude q
Dynamic scaling for time-dependent correlation functions in the vicinity of a critical point.
$\tilde{\Gamma}(q,\omega,t,h) \approx \frac{1}{q^{2-\eta}}\mathcal{G}(q^{-z}\omega, t^{\nu}\xi, h/t^{\Delta})$;

- z: dynamic critical exponent
- ω: frequency
- $\mathcal{G}$: a scaling function

Relaxation time τ diverges as

$$\tau \sim \xi^{z}.$$

Equal-Time Structure Functions

- Order-p, equal-time, structure functions:

$$\mathcal{S}_p(r) \equiv \langle [\delta u_{\|}(\vec{x}, \vec{r}, t)]^p \rangle \sim r^{\zeta_p}$$

$$\delta u_{\|}(\vec{x}, \vec{r}, t) \equiv [\vec{u}(\vec{x} + \vec{r}, t) - \vec{u}(\vec{x}, t)] \cdot \frac{\vec{r}}{r}$$

  η_d: Kolmogorov dissipation scale;
  L: large length scale at which energy is injected into the system.

- Experiments favour multiscaling: ζ_p a nonlinear, convex monotone increasing function of p.
- Simple-scaling prediction of Kolmogorov: $\zeta_p^{K41} = p/3$.

Introduction : Frames of Reference

- **Eulerian** :
  The Navier-Stokes equation is written in terms of the Eulerian velocity $\mathbf{u}$ at position $\mathbf{x}$ and time t. In the Eulerian case the frame of reference is fixed with respect to the fluid;
- **Lagrangian** :
  Frame of reference fixed to a fluid *particle*; this fictitious particle moves with the flow and its path is known as a Lagrangian trajectory.

$$\mathbf{v} = \left(\frac{d\mathbf{R}}{dt}\right)_{\mathbf{r_0}};$$

- **Quasi-Lagrangian** :
  It uses the following transformation for an Eulerian field $\psi(\mathbf{r}, t)$:

$$\hat{\psi}(\mathbf{r}, t) \equiv \psi[\mathbf{r} + \mathbf{R}(t; \mathbf{r_0}, 0), t].$$

Time-Dependent Structure Functions

- The order-p, time-dependent longitudinal structure function:

$$\mathcal{F}_p(r, \{t_1, \ldots, t_p\}) \equiv \langle [\delta u_{\|}(\vec{x}, t_1, r) \ldots \delta u_{\|}(\vec{x}, t_p, r)] \rangle$$

  For simplicity we consider $t_1 = t$ and $t_2 = \ldots = t_p = 0$.

- Given $\mathcal{F}(r, t)$, different ways of extracting time scales yield different exponents that are defined via dynamic-multiscaling ansätze:

$$\mathcal{T}_p(r) \sim r^{z_p}.$$

The GOY Shell Model

The evolution equation for the GOY shell model takes the form,

$$[\frac{d}{dt} + \nu k_n^2]u_n = i(a_n u_{n+1} u_{n+2} + b_n u_{n-1} u_{n+1} + c_n u_{n-1} u_{n-2})^* + f_n.$$

- In the shell model equation,
  - $k_n = k_0 2^n$, where $k_0 = 1/16$;
  - $a_n = k_n$, $b_n = -\delta k_{n-1}$, $c_n = -(1-\delta)k_{n-2}$, where $\delta = 1/2$.

Simulation Details

- We use the slaved Adams-Bashforth scheme to integrate the GOY shell model equation with 22 shells.
- We use $\delta t = 10^{-4}$ and $\nu = 10^{-7}$.
- For statistically steady turbulence, we use external forcing to drive the system.
- We study decaying turbulence by using two kinds of initial conditions:
  1. a random configuration where all the energy is concentrated at large length scales;
  2. a configuration obtained from a statistically steady turbulent state.

Details: Forced Turbulence

- We start from an initial condition where all the energy is concentrated in the large length scales, i.e., $v_n^0 = k_n^{-1/3} e^{i\theta_n}$ (for n = 1,2) and $v_n^0 = 0$ (for n = 3 to 22), with θ_n a random phase angle distributed uniformly between 0 and 2π.
- The system is then driven to a statistically steady state with a force $f_n = \delta_{n,1}(i + i) \times 5 \times 10^{-3}$.
- All measurements are made once the system reaches a statistically steady state.

Details: Decaying Turbulence

- For the first initial condition we use $v_n^0 = k_n^{1/2} e^{i\theta_n}$ (for n = 1,2) and $v_n^0 = k_n^{1/2} e^{-k_n{}^2} e^{i\theta_n}$ (for n = 3 to 22) with θ_n a random phase angle distributed uniformly between 0 and 2π.
- For the second initial condition, we first achieve a forced statistically steady state, with $f_n = \delta_{n,1}(i+i) \times 5 \times 10^{-3}$. The force is then switched off at some time origin t_0 and the system is allowed to decay freely.
- Our exponents are independent of the kind of initial condition we choose.

Error Estimates (GOY)

- Static solution exhibit a 3-cycle in the shell index n.
- Obtain 50 different values of each of the exponents from 50 independent simulations.
- Time-averaging is done over a time $T_{av} = 10^5 \times \tau_L$ to obtain the results for statistically steady state quantities. For decaying turbulence, we average over 20000 statistically independent initial configurations.
- The means of these 50 values for each of the dynamic-multiscaling exponents are shown in figure and the standard deviation yields error.
- This averaging is another way of removing the effects of the 3-cycle mentioned above.

Principal Results: Fluid Turbulence

- Simple dynamic scaling for Eulerian-velocity structure functions ($z_p^E = 1$).
- Dynamic multiscaling is obtained for Lagrangian or Quasi-Lagrangian structure functions.
- Dynamic multiscaling exponents z_p depend on how $\mathcal{T}_p(r)$ is extracted.
- z_p is related to the equal-time exponents via bridge relations.
- Universality of dynamic exponents: the same for decaying and statistically steady turbulence.

Integral Time Scale

- From the longitudinal, time-dependent, order-p structure functions, the order-p, degree-M, integral time scale is defined as,

$$\mathcal{T}^{I}_{p,M}(r) \equiv \left[\frac{1}{\mathcal{S}_p(r)}\int_0^\infty \mathcal{F}_p(r,t)t^{(M-1)}dt\right]^{(1/M)}$$

- The integral dynamic multiscaling exponent $z^{I}_{p,M}$ is defined as

$$\mathcal{T}^{I}_{p,M}(r) \sim r^{z^{I}_{p,M}}.$$

Derivative Time Scale

- Similarly, the order-p, degree-M derivative time scale is defined as

$$\mathcal{T}^{D}_{p,M}(r) \equiv \left[\frac{1}{\mathcal{S}_p(r)}\frac{\partial^M \mathcal{F}_p(r,t)}{\partial t^M}\right]^{(-1/M)}$$

- The derivative dynamic multiscaling exponent $z^{D}_{p,M}$ is defined as

$$\mathcal{T}^{D}_{p,M}(r) \sim r^{z^{D}_{p,M}}.$$

Theoretical Prediction

- The multifractal model predicts the following bridge relations:

$$z^{I}_{p,M} = 1 + \frac{[\zeta_{p-M} - \zeta_p]}{M};$$

$$z^{D}_{p,M} = 1 + \frac{[\zeta_p - \zeta_{p+M}]}{M}.$$

Extending the Frisch-Parisi Multifractal Model

Dynamic Structure Functions

$$\mathcal{F}_p(\ell, t) \propto \int_{\mathcal{I}} d\mu(h) (\frac{\ell}{L})^{\mathcal{Z}(h)} \mathcal{G}^{p,h}(\frac{t}{\tau_{p,h}}),$$

where $\mathcal{G}^{p,h}(\frac{t}{\tau_{p,h}})$ has a characteristic decay time $\tau_{p,h} \sim \ell/\delta v(\ell) \sim \ell^{1-h}$, and $\mathcal{G}^{p,h}(0) = 1$. If $\int_0^\infty t^{(M-1)} \mathcal{G}^{p,h} dt$ exists, then the order-p, degree-M, integral time scale is

$$\mathcal{T}^I_{p,M}(\ell) \equiv \left[\frac{1}{\mathcal{S}_p(\ell)} \int_0^\infty \mathcal{F}_p(\ell, t) t^{(M-1)} dt \right]^{(1/M)}.$$

* V.S. L'vov, E. Podivilov, and I. Procaccia, Phys. Rev. E **55**,7030 (1997).

Multifractal Model

$$\mathcal{T}^{I}_{p,1}(\ell) \equiv \left[\frac{1}{\mathcal{S}_p(\ell)}\int_0^\infty \mathcal{F}_p(\ell,t)dt\right]^{(1/M)}$$

$$\propto \left[\frac{1}{\mathcal{S}_p(\ell)}\int_{\mathcal{I}} d\mu(h)(\frac{\ell}{L})^{\mathcal{Z}(h)}\int_0^\infty dt\mathcal{G}^{p,h}(\frac{t}{\tau_{p,h}})\right]$$

$$\propto \left[\frac{1}{\mathcal{S}_p(\ell)}\int_{\mathcal{I}} d\mu(h)(\frac{\ell}{L})^{ph+3-D(h)}\ell^{1-h}\right]$$

In the last step, we have used :

$$\tau_{p,h} \sim \ell/\delta v(\ell) \sim \ell^{1-h}$$

Multifractal Model

- Corresponding Bridge Relations :

$$z^{I}_{p,1} = 1 + [\zeta_{p-1} - \zeta_p],$$

$$z^{D}_{p,2} = 1 + [\zeta_p - \zeta_{p+2}]/2.$$

- Bridge relations reduce to $z_p^{K41} = 2/3$ if we assume K41 scaling for the equal-time structure functions.

Numerical studies of dynamic multiscaling

- L. Biferale, G. Bofetta, A. Celani, and F. Toschi, Physica D **127** 187 (1999); this study uses an exit-time method.
- Our group has concentrated on an elucidation of dynamic multiscaling by using time-dependent structure functions and
  (a) shell models and
  (b) the two-dimensional Navier-Stokes equation with friction.

In the following slides we give an overview of our results without technical details.

Results

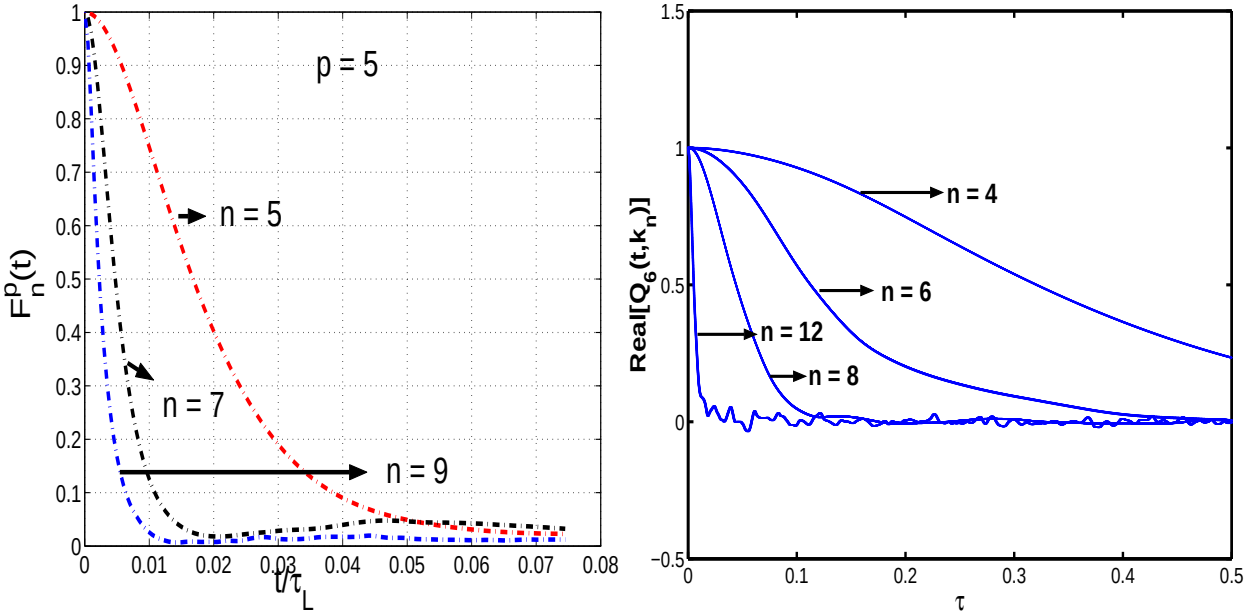

Plots of order-p structure functions *vs* the dimensionless time for various shells for statistically steady (left) and decaying (right) turbulence.

Integral Time Scales

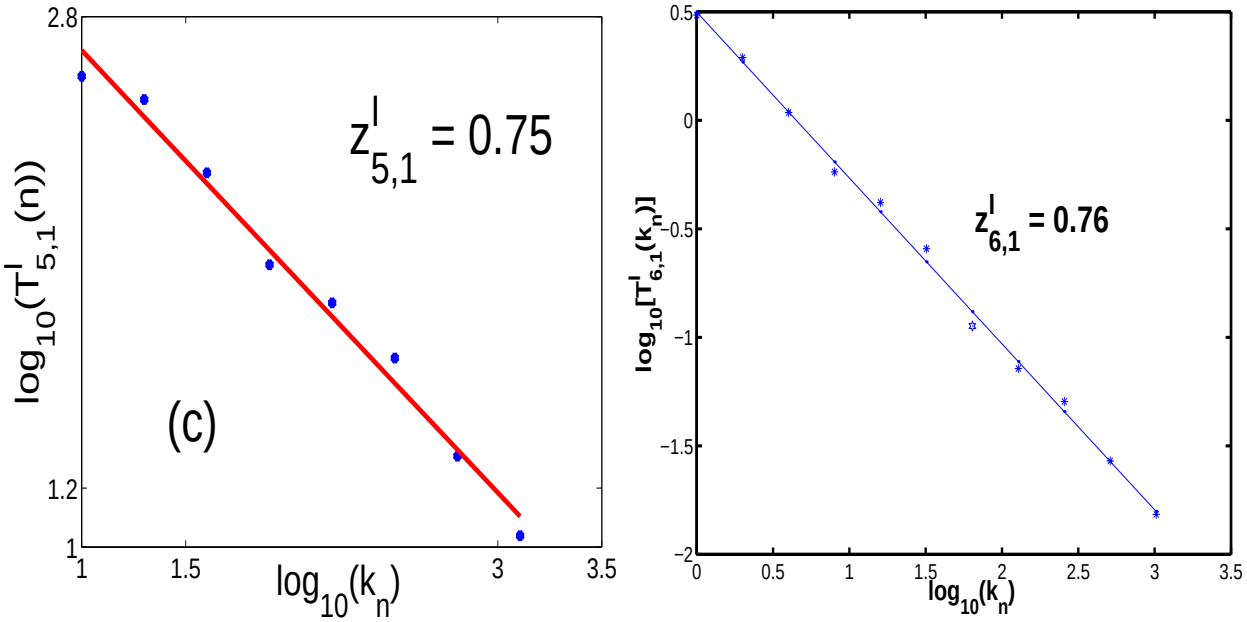

Log-log plots of integral times for statistically steady (left) and decaying (right) turbulence for order-p structure functions; the slopes of these graphs yield $z^I_{p,1}$. The integration is carried out over time 0 to t_u, where we choose t_u such that $F_p(n, t_u)$ (or $Q_p(n, t_u)) = \alpha$ for all n and p.

Derivative Time Scales

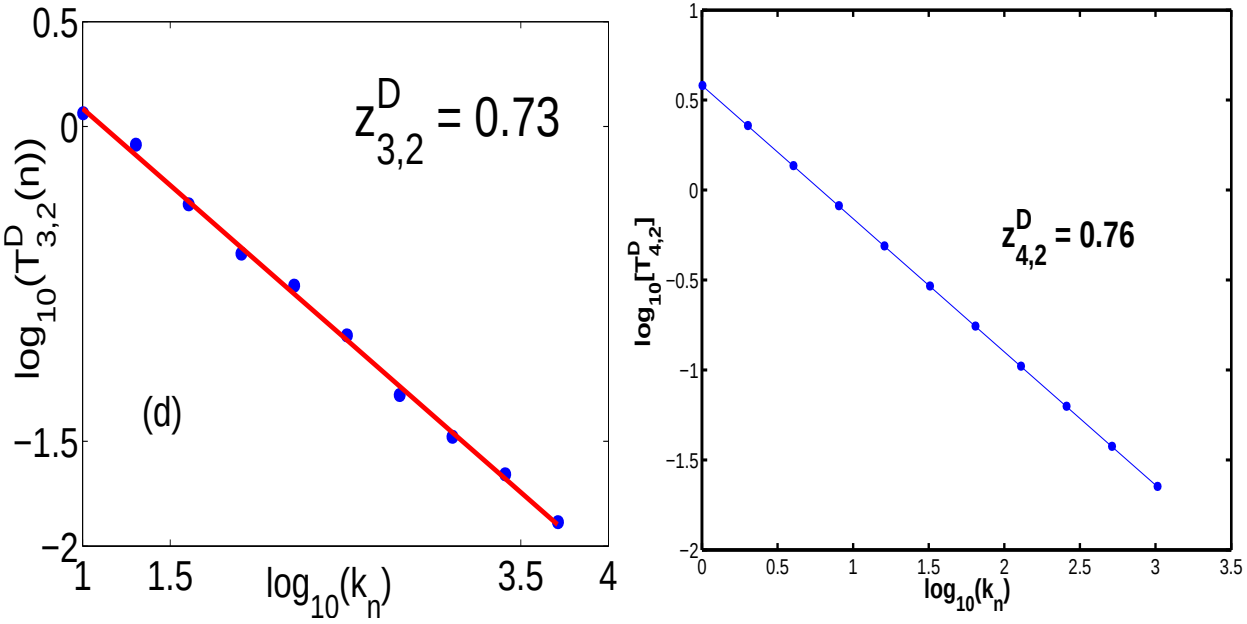

The analogue of the previous figure for derivative time scales yields $z^D_{p,1}$. We use a centered, sixth-order, finite-difference scheme by extending $F_p(n,t)$ (or $Q_p(n,t)$) to negative t via $F_p(n,-t)$(or $Q_p(n,-t)) = F_p(n,t)$(or $Q_p(n,t)$) to obtain the derivative time scales.

Passive Scalars

- We use two different kinds of velocity fields in the advection-diffusion equation for both statistically steady and decaying turbulence:
  - Model A : The Kraichnan ensemble where each component of $\mathbf{u}$ is a zero-mean, delta-correlated Gaussian random variable.
  - Model B : Velocities from the GOY shell model.

Principal Results: Passive-Scalars

- Dynamic multiscaling is obtained only if the advecting velocity is intermittent.
- Simple dynamic scaling is obtained for a simple version of the passive-scalar problem (Kraichnan), in which the advecting velocity field is Gaussian, even though equal-time structure functions display multiscaling in this model.
- For intermittent velocity fields, different time scales can be extracted.
- z_p related to ζ_p through bridge relations.
- Universality: Dynamic exponents for decaying and statistically steady passive-scalar turbulence are equal.

Model A

- The covariance of the field is

$$< u_i(\mathbf{x}, t) u_j(\mathbf{x} + \mathbf{r}, t') >= 2D_{ij}\delta(t - t')$$

where the Fourier Transform of D_{ij} has the form

$$\tilde{D}_{ij}(\mathbf{q}) \propto \left(q^2 + \frac{1}{L^2}\right)^{-(d+\xi)/2} e^{-\eta q^2} \left[\delta_{ij} - \frac{q_i q_j}{q^2}\right].$$

In the limits $L \Gamma\rightarrow \infty$ and $\eta \Gamma\rightarrow 0$, D_{ij} in real space is

$$D_{ij}(\mathbf{r}) = D^0 \delta_{ij} - \frac{1}{2} d_{ij}(\mathbf{r}))$$

where,

$$d_{ij} = D_1 r^{\xi} \left[(d - 1 + \xi)\delta_{ij} - \xi \frac{r_i r_j}{r^2}\right]$$

Passive-scalar shell models

$$\left[\frac{d}{dt} + \kappa k_n^2\right]\theta_n = \imath\Big[a_n(\theta^*_{n+1}u^*_{n-1} - \theta^*_{n-1}u^*_{n+1}) + b_n(\theta^*_{n-1}u^*_{n-2} + \theta^*_{n-2}u_{n-1}) + c_n(\theta^*_{n+2}u_{n+1} + \theta^*_{n+1}u^*_{n+2})\Big] + f_n,$$

where the asterisks denote complex conjugation, $a_n = k_n/2$, $b_n = -k_{n-1}/2$, and $c_n = k_{n+1}/2$; f_n is an additive force that is used to drive the system to a steady state; the boundary conditions are $u_{-1} = u_0 = \theta_{-1} = \theta_0 = 0; u_{N+1} = u_{N+2} = \theta_{N+1} = \theta_{N+2} = 0$.

- For the Kraichnan model, the advecting velocity variables are taken to be zero-mean, white-in-time, Gaussian random complex variables with covariance $\langle u_n(t)u^*_m(t')\rangle = C_2 k_n^{-\xi}\delta_{mn}\delta(t-t')$.
- For a "turbulent" passive-scalar field, the advecting velocity field is a solution of the GOY shell model.

Model A

This model shows multiscaling for equal-time passive-scalar structure functions for $0 < \xi < 2$.

Dynamic Multiscaling in Passive-Scalars

Multifractal model predicts:

- $z^D_{p,M} = 1 - \zeta^u_M / M$
- $z^I_{p,M} = 1 - |\zeta^u_{-M}| / M$
- Breakdown of simple scaling.
- Does structure functions with negative exponents exists?

Analytical and Numerical Results

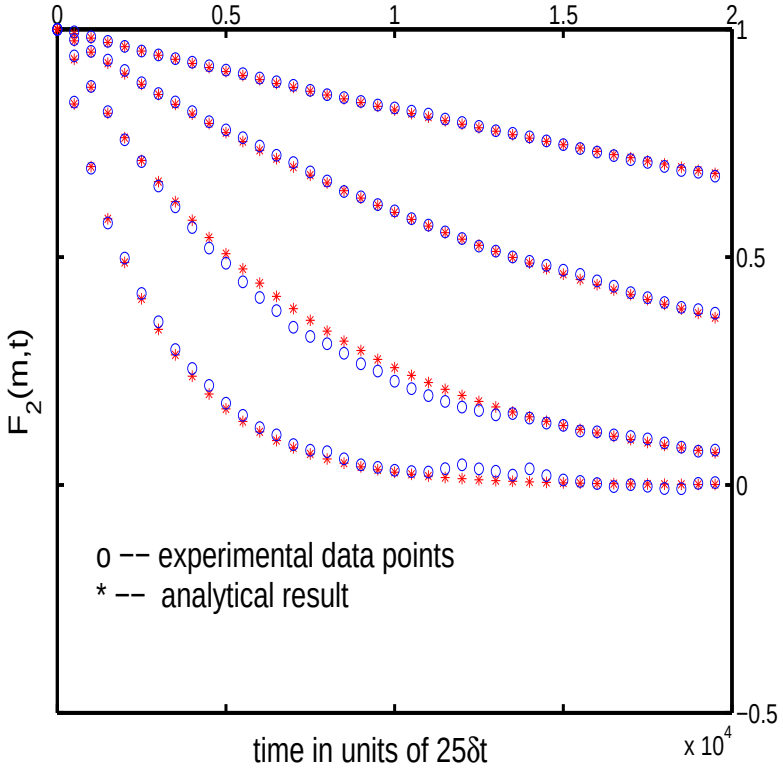

A comparison of our numerical and analytical results for model A second-order structure function in decaying turbulence.

Model A: Numerical Results

- Analytical work shows that for Model A the time-dependent structure functions decay exponentially.
- A log-log plot of the characteristic decay time *vs* the wave vectors yield the dynamic exponent z_p.
- It is shown analytically that for all order-p time-dependent structure functions, $z_p = 2 - \xi$.
- Our numerics support this prediction for decaying passive-scalar fields.

Model A: Numerical Results

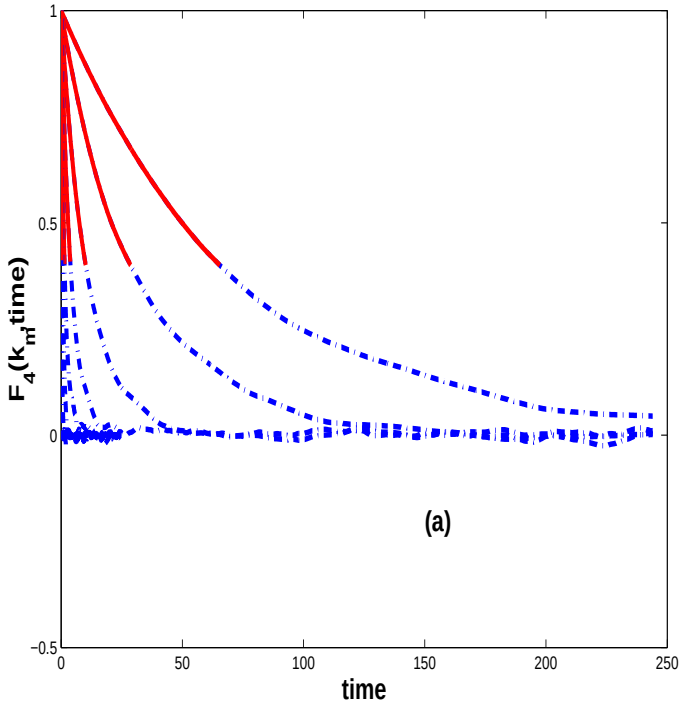

A plot of the fourth-order structure function ($\xi = 0.6$) *vs* time for statistically steady turbulence. The scaling exponent is extracted from the decay constant of the curves.

Model A: Numerical Results

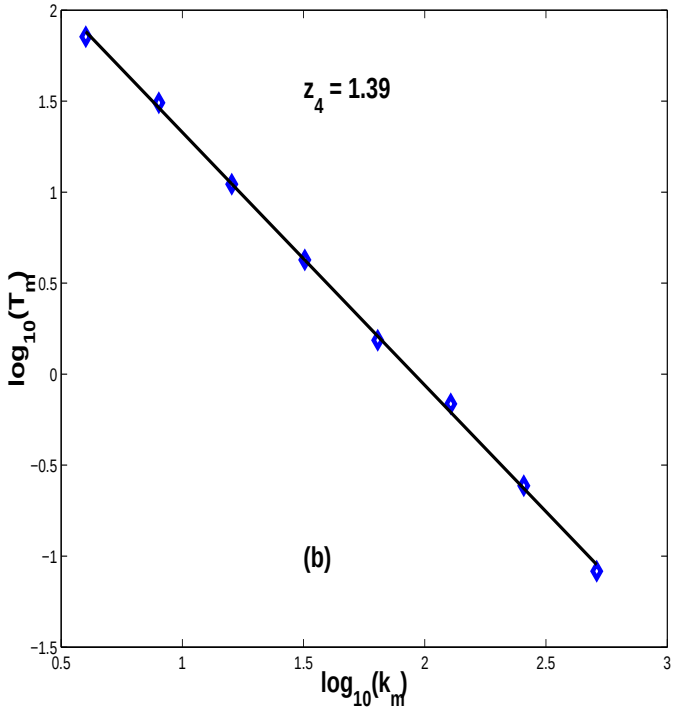

The slope of a log-log plot of the decay constant *vs* the wave-vector yields the dynamic scaling exponent for the fourth-order structure function.

Model A: Numerical Results

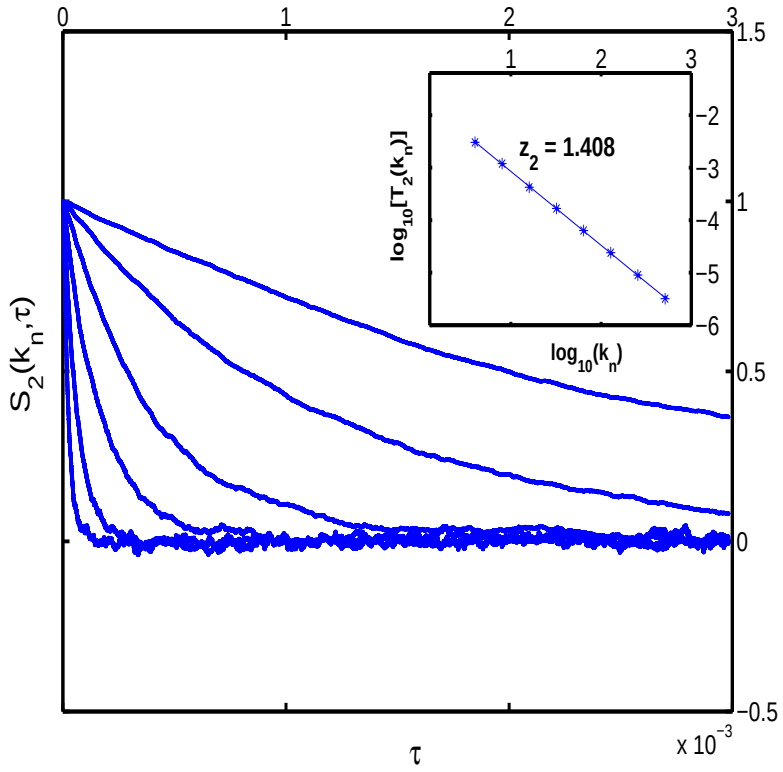

A plot of the second-order dynamic structure function for decaying turbulence. The slope of a log-log plot (inset) of the decay time *vs* the wave-vector yields the dynamic exponent .

Model B: Numerical Results

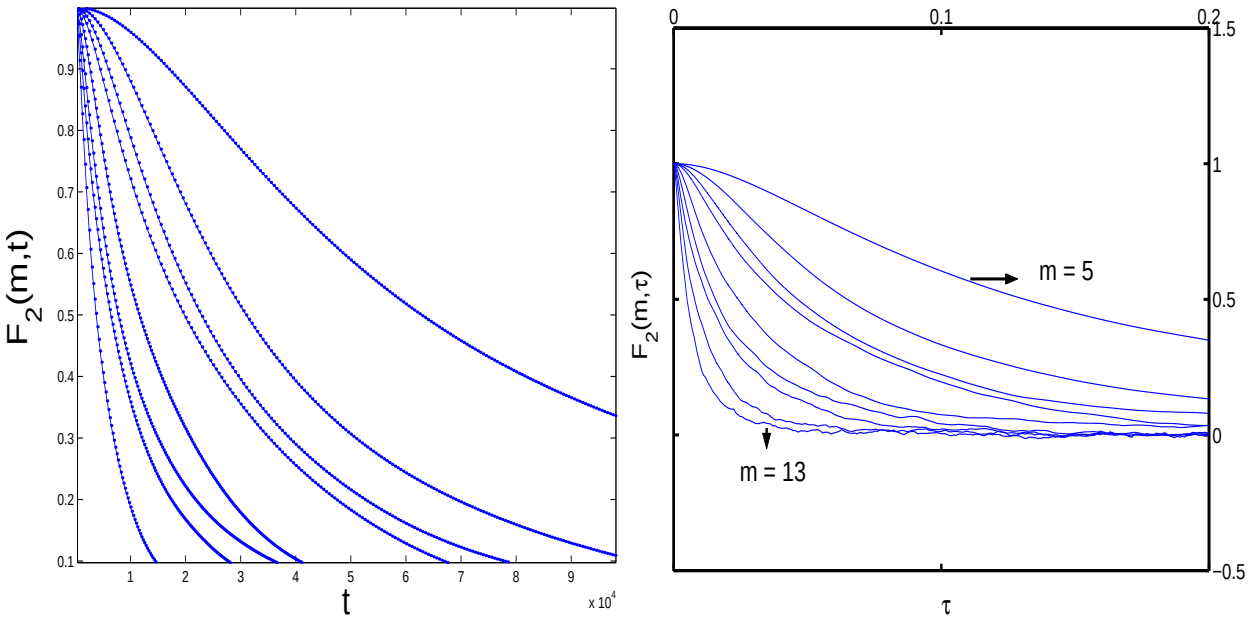

Plots of the second-order time-dependent structure function *vs* the dimensionless time for statistically steady (left) and decaying turbulence (right).

Cumulative pdf for u_m

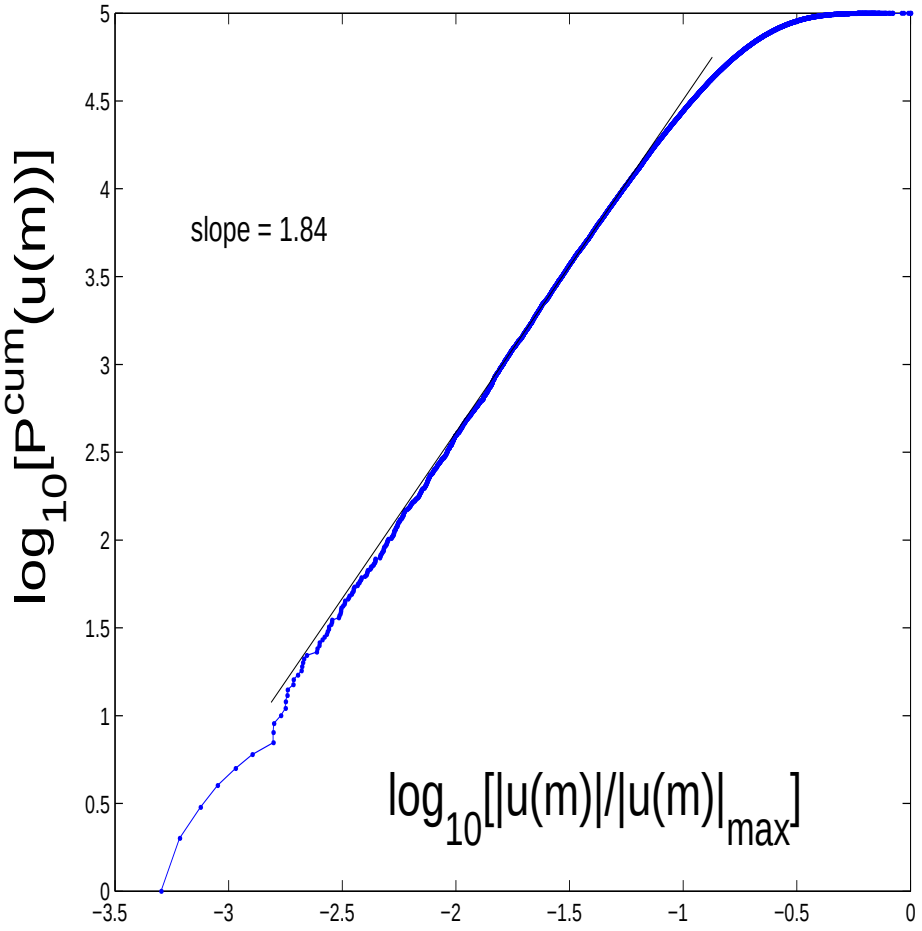

Negative Exponents

- For small $|u_m|$, $P^{cum}[|u_m|] \sim |u_m|^{1.8}$.
- $P[|u_m|] \sim |u_m|^{0.8}$.
- $S_{-1}(m) \equiv \int P[x]\frac{1}{x}dx \sim \int x^{-0.2}dx$ exists.
- But $S_p(m)$ for $p \approx -1.8$ does not.
- $T^I_{p,M}$ for $M > 2$ does not exist.
- Measurement of a static quantity $(P(x))$ gives us information about existence of a dynamic quantity $T^I_{p,M}$.

Model B: Integral Time Scale

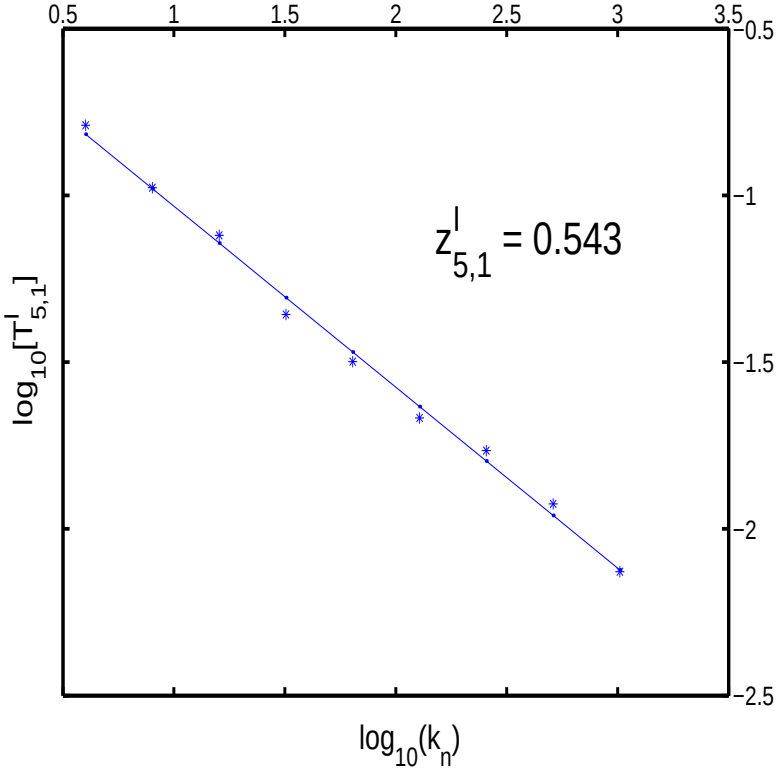

A log-log plot of the integral time scale *vs* the wave-vector in decaying turbulence. The linear fit gives us the scaling exponent $z^I_{p,M}$.

Derivative Time Scale

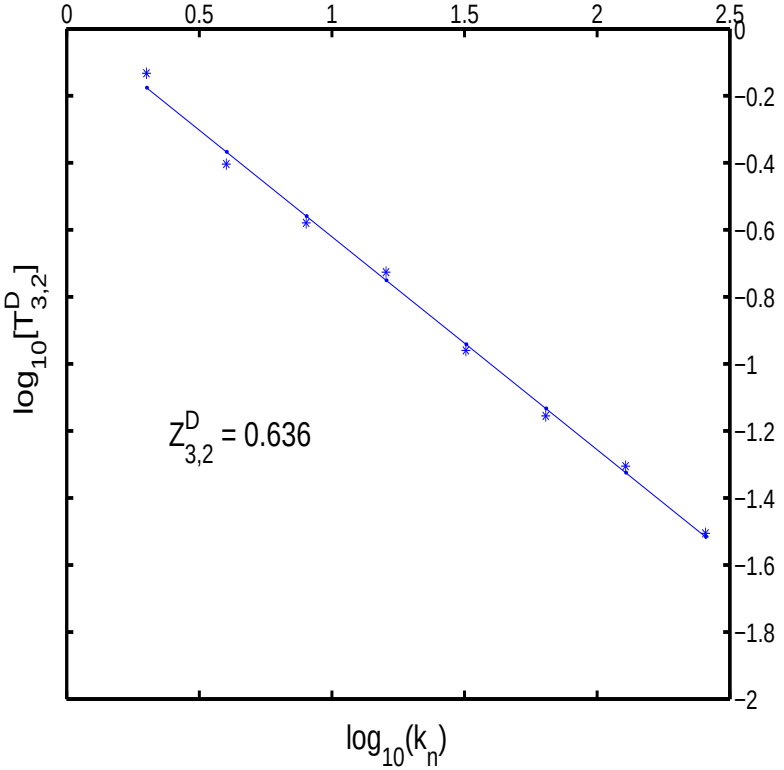

A log-log plot of the derivative time scale *vs* the wave-vector in decaying turbulence. The linear fit gives us the scaling exponent $z^D_{p,M}$.

Exponents for dynamic multiscaling in shell models

order(p)	ζ_p^u	$z_{p,1}^{I,u}$[Theory]	$z_{p,1}^{I,u}$	$z_{p,2}^{D,u}$[Theory]	$z_{p,2}^{D,u}$
1	0.379 ± 0.008	0.621 ± 0.008	0.61 ± 0.03	0.68 ± 0.01	0.699 ± 0.008
2	0.711 ± 0.002	0.66 ± 0.01	0.68 ± 0.01	0.716 ± 0.008	0.723 ± 0.006
3	1.007 ± 0.003	0.704 ± 0.005	0.711 ± 0.001	0.74 ± 0.01	0.752 ± 0.005
4	1.279 ± 0.006	0.728 ± 0.009	0.734 ± 0.002	0.76 ± 0.02	0.76 ± 0.01
5	1.525 ± 0.009	0.75 ± 0.02	0.755 ± 0.002	0.77 ± 0.02	0.77 ± 0.02
6	1.74 ± 0.01	0.78 ± 0.02	0.78 ± 0.03	0.77 ± 0.03	0.78 ± 0.02

order(p)	ζ_p^θ	$z_{p,1}^{I,\theta}$	$z_{p,2}^{D,\theta}$
1	0.342 ± 0.002	0.522 ± 0.002	0.632 ± 0.003
2	0.634 ± 0.003	0.531 ± 0.004	0.647 ± 0.003
3	0.873 ± 0.003	0.553 ± 0.006	0.646 ± 0.003
4	1.072 ± 0.004	0.563 ± 0.003	0.642 ± 0.005
5	1.245 ± 0.004	0.562 ± 0.006	0.643 ± 0.006
6	1.370 ± 0.006	0.576 ± 0.006	0.640 ± 0.005

Multiscaling and quasi-Lagrangian Structure Functions in 2D flows

- Multiscaling in equal-time, Eulerian vorticity structure functions.
- Investigating dynamic-multiscaling in time-dependent, quasi-Lagrangian vorticity structure functions.
- Tracking a single particle in a $2D$ flow with friction to generate quasi-Lagrangian fields.

Movie

Steady State quasi-Lagrangian Vorticity Field

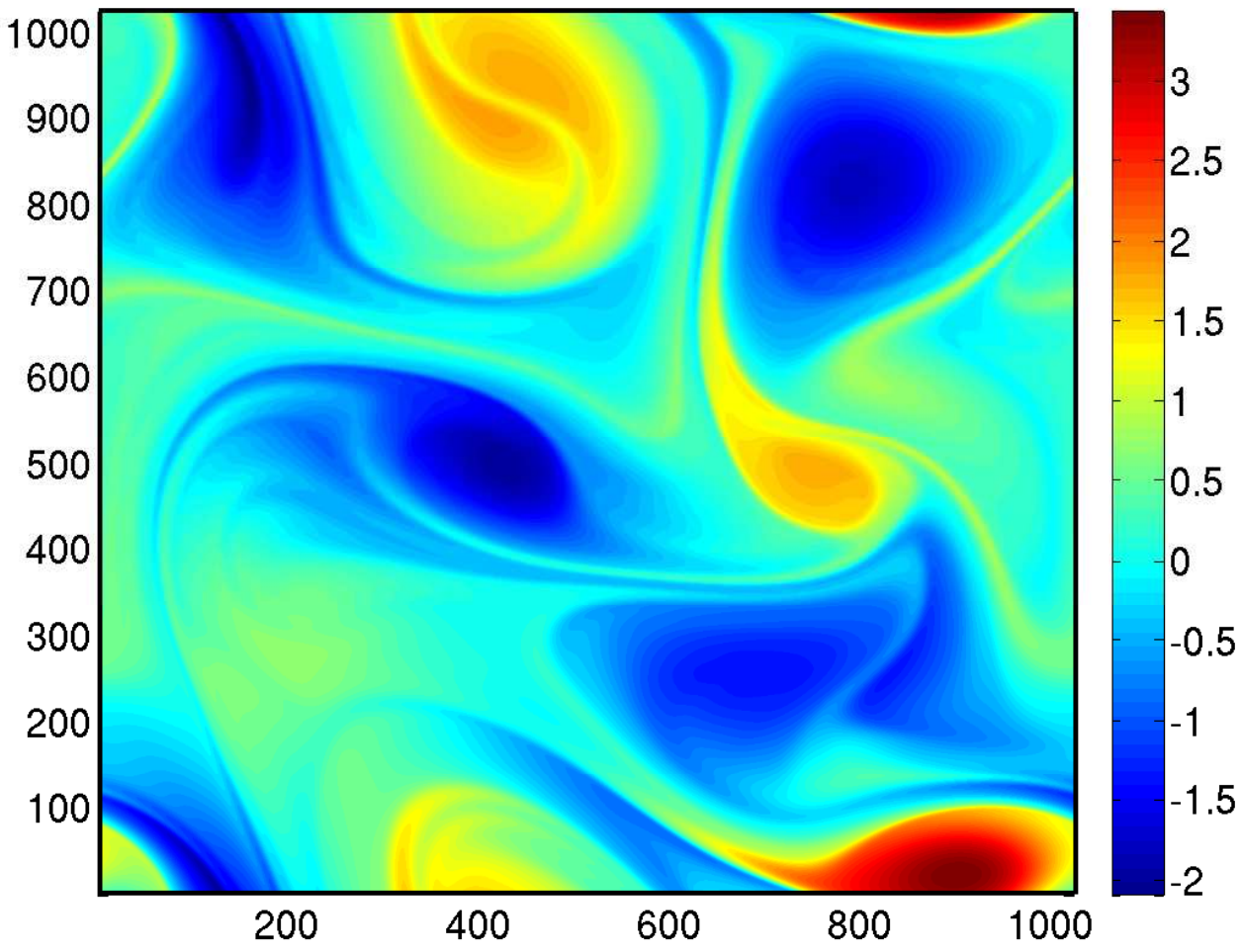

A pseudocolor plot of the quasi-Lagrangian vorticity field in the statistically steady state.

Equal-time Structure Functions

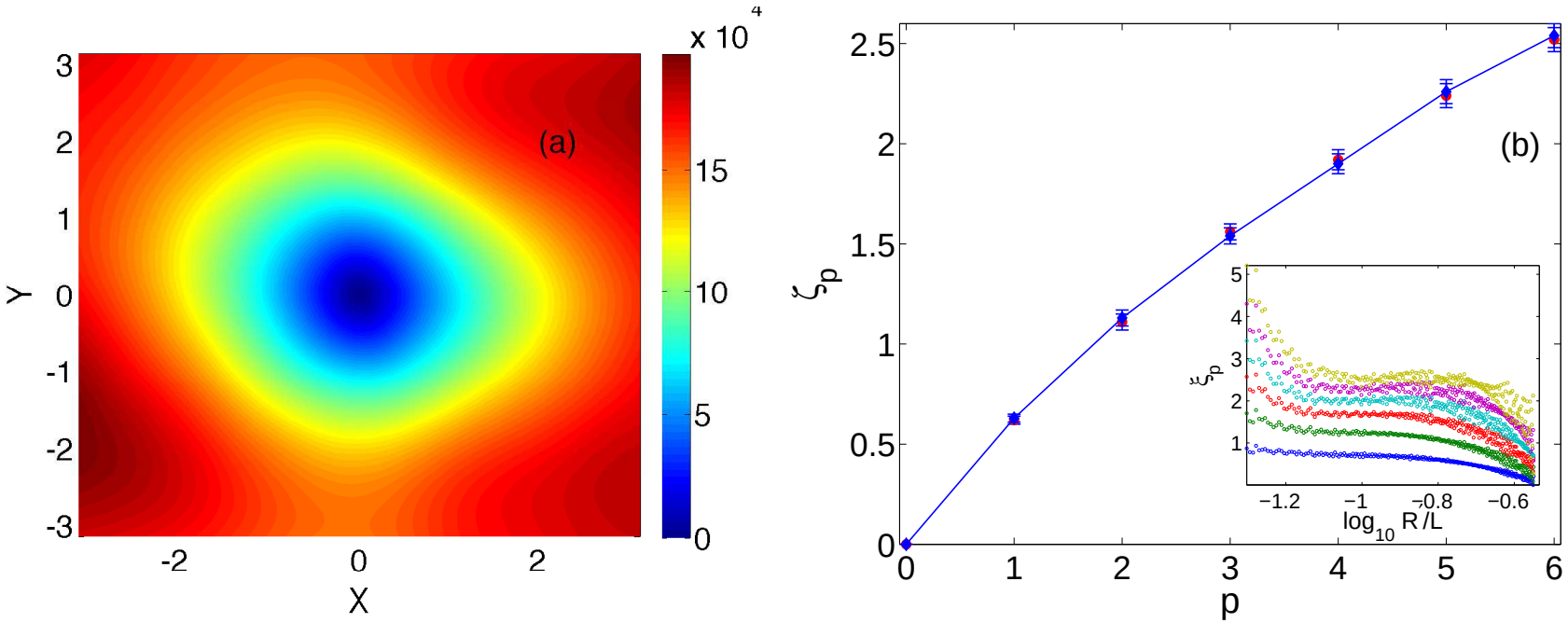

- Left : $S_3^{\omega}(\mathbf{R})$ for the quasi-Lagrangian field, obtained by averaging over the centers r_c.
- Right : Scaling exponents for equal-time, vorticity structure functions, for both the Eulerian and quasi-Lagrangian fields.

Time-dependent Structure Functions

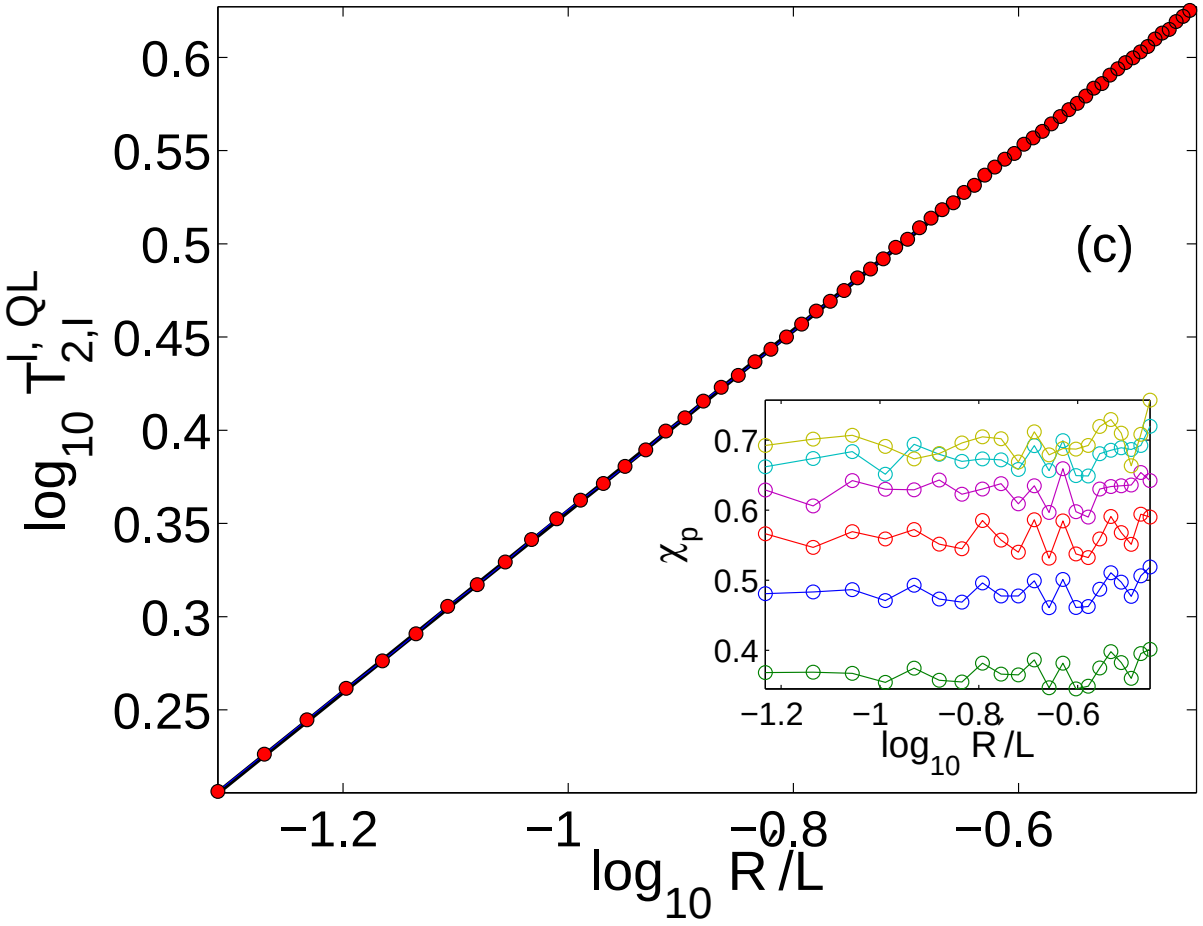

A loglog plot of $T^{l}_{2,1}$ versus the separation r; the data points are shown by open red circles and the straight black line shows the line of best fit in the inertial range.

Effect of Friction

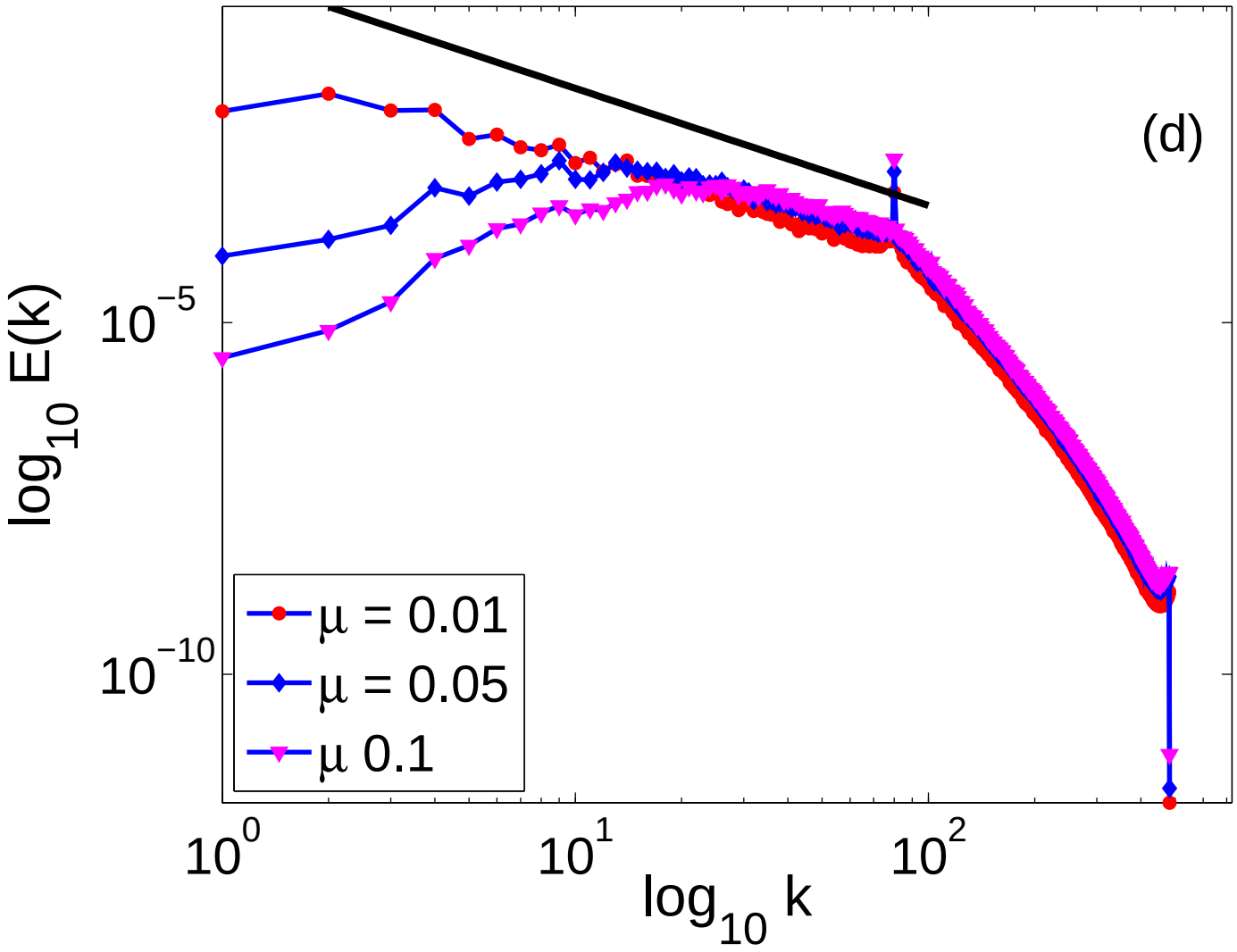

A log-log plot of the energy spectrum versus the wavevector k for various values of μ.

Time-dependent multiscaling exponents

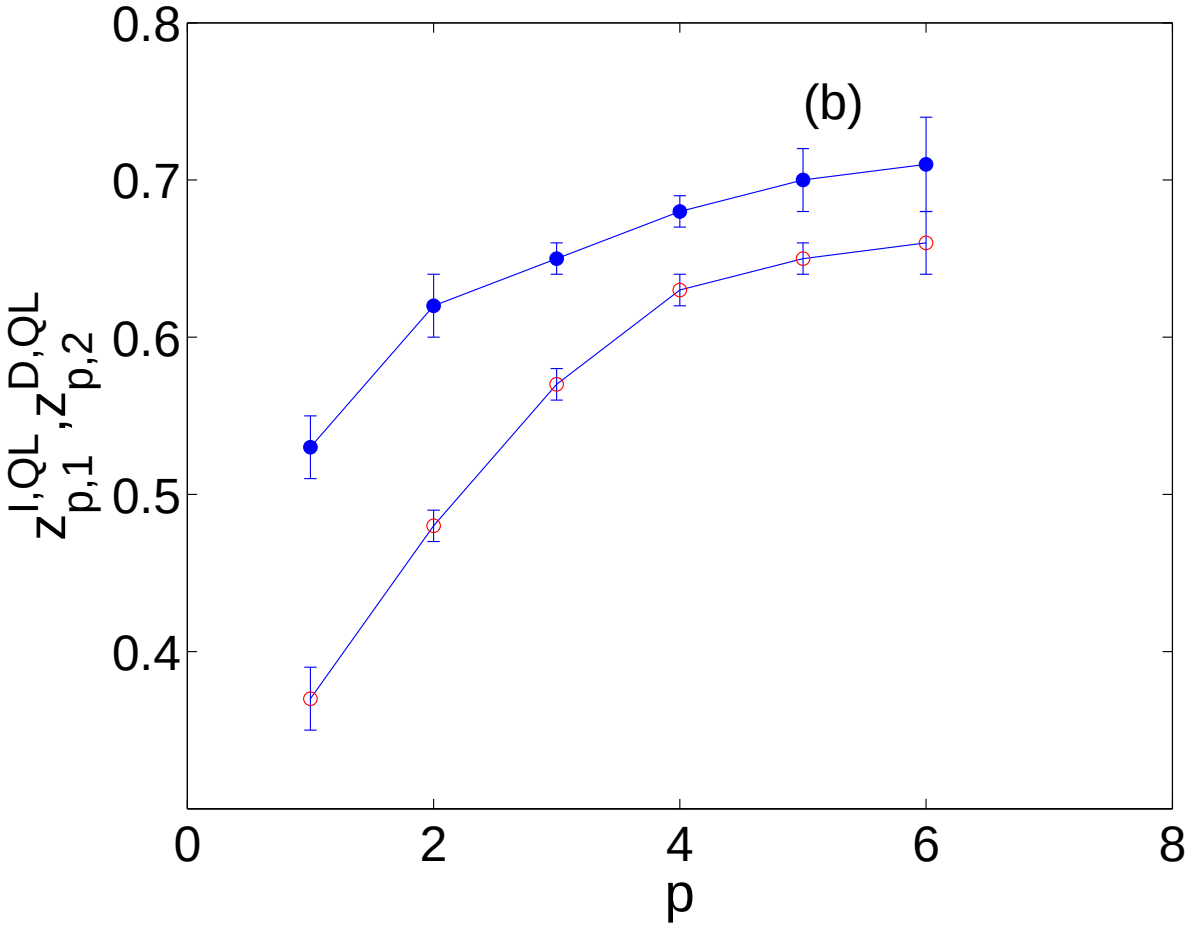

Plots of the vorticity, dynamic-multiscaling, quasi-Lagrangian exponents $z_{p,1}^{I,\mathrm{QL}}$ (open red circles) and $z_{p,2}^{D,\mathrm{QL}}$ (full blue circles) versus p with the error bars

Exponents from 2D DNS

order(p)	ζ_p^{qL}	$z_{p,1}^{l,\mathrm{qL}}$[Theory]	$z_{p,1}^{l,\mathrm{qL}}$	$z_{p,2}^{D,\mathrm{qL}}$[Theory]	$z_{p,2}^{D,\mathrm{qL}}$
1	0.625 $\pm$ 0.003	0.375 $\pm$ 0.007	0.37 $\pm$ 0.02	0.541 $\pm$ 0.008	0.53 $\pm$ 0.02
2	1.131 $\pm$ 0.005	0.49 $\pm$ 0.02	0.48 $\pm$ 0.01	0.618 $\pm$ 0.009	0.62 $\pm$ 0.2
3	1.541 $\pm$ 0.005	0.58 $\pm$ 0.01	0.57 $\pm$ 0.01	0.66 $\pm$ 0.01	0.67 $\pm$ 0.01
4	1.895 $\pm$ 0.004	0.65 $\pm$ 0.01	0.65 $\pm$ 0.01	0.675 $\pm$ 0.008	0.66 $\pm$ 0.03
5	2.222 $\pm$ 0.008	0.67 $\pm$ 0.01	0.65 $\pm$ 0.02	0.70 $\pm$ 0.01	0.70 $\pm$ 0.02
6	2.544 $\pm$ 0.004	0.68 $\pm$ 0.01	0.66 $\pm$ 0.02	0.71 $\pm$ 0.02	0.71 $\pm$ 0.03

Conclusions

- The calculation of dynamic-multiscaling exponents has been limited so far to shell models for 3D, homogeneous, isotropic fluid and passive-scalar turbulence.
- We have presented the first study of such dynamic multiscaling in the direct-cascade régime of 2D fluid turbulence with friction by calculating both quasi-Lagrangian and Eulerian structure functions.
- Our work brings out clearly the need for an infinity of time scales and associated exponents to characterize such multiscaling; and it verifies, within the accuracy of our numerical calculations, the linear bridge relations for a representative value of μ.
- We find that friction also suppresses sweeping effects so, with such friction, even Eulerian vorticity structure functions exhibit dynamic multiscaling with exponents that are consistent with their quasi-Lagrangian counterparts.